Advances in Colloid and Interface Science, 10 (1979) 173—214

COMPUTER EXPERIMENTS ON PHASE SEPARATION IN BINARY ALLOYS[†]

K. BINDER
Universitat des Saarlandes, Saarbrucken, Germany
M.H. KALOS
Courant Institute of Mathematical Science, New York University, New York, New York 10012, U.S.A.
J.L. LEBOWITZ AND J. MARRO[††]
Belfer Graduate School of Science, Yeshiva University, New York, New York 10033 U.S.A.

CONTENTS

INTRODUCTION

A binary alloy, such as ZnAℓ, is spatially homogeneous when it is in thermal equilibrium at sufficiently high temperatures; that is, it consists of one thermodynamic phase. If the system is suddenly quenched to a lower temperature (see Fig. I), it remains spatially homogeneous. Thermal equilibrium, however, requires the coexistence of two phases, one A-rich and one B-rich, whenever the fraction of "B-atoms" $\bar{c}$ is in the range $c_A < \bar{c} < c_B$ in Fig. I. The nature of the time evolution

[†]Work supported by AFOSR Grant No. 73-2430B and E.R.D.A. Contract No. AT(11-1)-3077.
[††]Permanent address: Departamento de Física Teórica, Universidad de Barcelona, and Instituto de Física Teórica del C.S.I.C., Barcelona-14, Spain. Partially supported by the Program for Cultural Interchange between Spain and the U.S.A. and the Fulbright-Hays Program, Madrid, Spain.

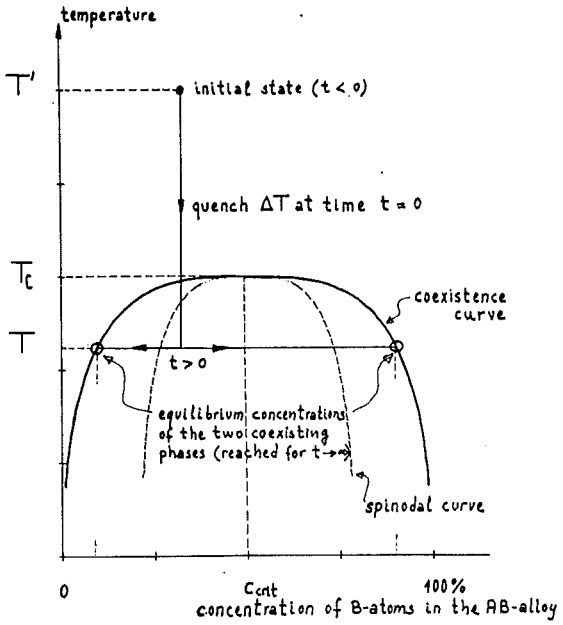

Fig. 1. Schematic phase diagram of a binary alloy with a miscibility gap. The time evolution of the quenched system is also indicated.

of the system after the quench is a problem of great practical interest in metallurgy. It also presents a challenge to the theorist. We first briefly summarize some of the main ideas and problems of the classical theory of this process.

According to the classical (Cahn-Hilliard) theory (ref. 1-3), one has to distinguish two regimes of different kinetic behavior. If the quench is to a state within the so-called *spinodal curve* (see Fig. 1), the system is supposed to be unstable with respect to *weak delocalized* (i.e., long wavelength) fluctuations; the growth of these fluctuations into zones of the two coexisting phases is called the *spinodal decomposition* mechanism. For states between the spinodal curve and the coexistence curve, the system is stable with respect to these delocalized fluctuations, but still unstable with respect to *strong localized* fluctuations (i.e., nucleus formation). Phase separation is then a consequence of the *nucleation* mechanism, considered extensively in the other chapters of this volume. After microdomains have been built up by some mechanism, these domains grow further (*coarsening of grains*). This coarsening may proceed by single atom processes where larger grains grow at the expense of smaller ones which are dissolved in the matrix (*Ostwald ripening* of the grains [ref. 4,5], as treated by the Lifshitz-Slyozov [ref. 6] theory), or by effective diffusion and coagulation of the grains (ref. 7) (as first considered in the *Smoluchowski coagulation* [ref. 8]

of raindrops in the atmosphere). In Fig. 1, $\bar{c}$ is arbitrarily chosen closer to c_A than to c_B so that the droplets grow primarily by agregation of B atoms in a background of A-rich phase.

While these ideas certainly give much insight into what is happening, a full theoretical treatment of this process should be expected to yield not only qualitative notions of the relaxation mechanism, but also quantitative estimates of the relaxation rates. This latter task leads to severe problems (ref. 9-19). Some of the open questions are:

1. The theory of spinodal decomposition (ref. 1-3) is based on the concept of a local free-energy density function (depending on the local concentration) for nonequilibrium states, but even the appropriate definition, let alone the explicit construction, of such a function encounters serious difficulties. Indeed, the existence of a well defined spinodal curve which usually derives from this free energy is questionable (ref. 9,16,17). Rather, there may be a continuous transition between spinodal decomposition and nucleation (ref. 2,16), especially in alloys. (In the case of long range interactions, however, nucleation rates can become arbitrarily small and the spinodal line can be given a well defined meaning (ref. 1B,19).

2. Even if this free energy is given, the derivation of closed kinetic equations describing the time evolution requires further assumptions and approximations (ref. 10-12).

3. The treatment of the resulting nonlinear equations describint the kinetic evolution of the system is difficult (ref. 10-15).

4. In the critical region ($T \to T_c$ and concentration near c_{crit}; see Fig. 1), a complicated interplay of the relaxation mechanisms with critical fluctuations may occur, which needs a separate study (ref. 7).

5. The regime of validity of descriptions of the asymptotic relaxation, $t \to \infty$, is unknown. The Lifshift-Slyozov theory (ref. 6) considers the coarsening in the case where the difference between the average concentration, $\bar{c}$, and the concentration at the coexistence curve, c_A, is very small, and it may break down the larger concentration differences.

6. A particularly difficult problem arises if well separated grains can no longer be distinguished, and one has a rather irregular "network" of interpenetrating zones. This regime should probably be treated from the point of view of "percolation theory" (ref. 20-27). That theory, however, usually considers only random mixing of two species A,B, and only very few studies take particle interactions into account (ref. 22).

Since some of these problems are the same as those which hamper the progress of the liquid-vapor nucleation theory, a more general study of phase separation kinetics will help elucidate that phenomenon as well. For the construction of such a theory, we need more quantitative information about the nature of the cooperative microscopic processes going on during phase separation. For reasons

explained in the next section, some of this information is best provi computer simulation of simple model systems (ref. 23-26, 14). These experiments and their implications for the theory are the subject of

The outline of this article is as follows: In the second section, brief review of some relevant experiments on phase separation kinetic: be pointed out that insufficient knowledge of the microscopic propert samples and complicated effects influencing the kinetics make a meani ison with theory very difficult. In the third section, the theoretic: mentioned earlier are described more fully and their quantitative pre reviewed. The fourth section describes the lattice models used in th simulation; sites of a rigid lattice are occupied by two kinds of ato boring atoms are interchanged according to a transition probability w detailed balance and an approach to the final thermal equilibrium sta fifth section, we then give some details of the computational techniq selection of the numerical results obtained (ref. 23-26,14). In the l we give our conclusions concerning the validity of the various theori

We are well aware that the "kinetic Ising model" of Kawasaki (ref. in our computer simulations, is a great oversimplification of nature occurs indirectly via vacancies, etc., rather than directly, and where misfits" of the two kinds of atoms (and resulting elastic distortions be taken into account. We nevertheless believe that the results of t simulation provide a stringent test of theories: If a theory fails to this very simple model, there is no reason to assume that it will wo for more complicated real systems!

EXPERIMENTAL SITUATION

Typical examples of the systems we have in mind are binary alloys etc. Since the scattering length of the two kinds of atoms in the al usually (e.g., in ZnAℓ) sufficiently different both for x-ray and neu the structure factor $S(\underline{k},t)$ may be determined experimentally. This f proportional to the intensity scattered with momentum transfer $\underline{k}$; it as the Fourier transform of the (spatial) concentration correlation f

$$S(\underline{k},t) = \sum_{\underline{r}} e^{i\underline{k}\cdot\underline{r}}\, G(\underline{r}\cdot t),$$

where

$$G(\underline{r},t) = \langle (c(\underline{r}';t) - \bar{c})(c(\underline{r}' + \underline{r},t) - \bar{c})\rangle .$$

Here, $c(\underline{r},t)$ is the fractional concentration of the B-component at po and time t. If we assume further, as is generally done, that the tot

density remains constant, then $c(\underline{r},t)$ also yields the different atom densities at $\underline{r}$ and t. The bracket $\langle\ \rangle$ indicates an average over $\underline{r}'$ in the macroscopic system; note that $\bar{c} \equiv \langle c(\underline{r},t)\rangle$ is constant during the temporal evolution. In most cases, activation energies for the diffusion of atoms in the lattice are high enough so that the coarsening proceeds on a macroscopic time scale. Therefore, one may take "snapshot pictures" of the state of the system with the radiation neglecting the variation of $S(\underline{k},t)$ with t during the picture taking time. In practice, one lets the system evolve up to some time t after the quench to the chosen temperature and then rapidly quenches the system to a much lower temperature where the scattering experiment is performed. The variation of $S(\underline{k},t)$ with time during (and after) this second quench can be neglected.

An example is presented in Fig. 2, where experimental results of Rundman and

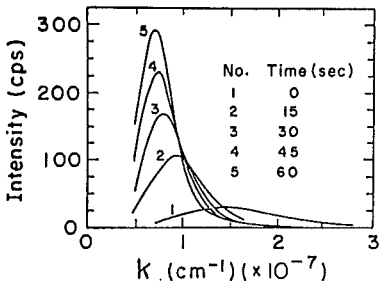

Fig. 2. X-ray spectra from ZnAℓ-alloys quenched and annealed for relatively long times at 100°C ($\simeq 0.7T_c$). The structure function $S(\underline{k},t)$ is plotted versus k (from ref. 28).

Hilliard (ref. 28) are shown for a ZnAℓ system quenched to around 100°C and annealed there during some interval of time, after which it was cooled to very low temperatures so that the state of the system was frozen in. If one neglects short range order, the initial state in Fig. 2 would correspond to a horizontal straight line. It is seen that a maximum develops, which grows steadily and is also slowly shifted to smaller values of the momentum transfer.

The position of the maximum may be related to the typical linear dimension of the zones which are precipitated in the coarsening process. Much interest has been devoted to the growth law of the zone mean radius, $\bar{R}$. Since, due to resolution problems, it is hard to observe the later stages of the coarsening by x-ray or neutron scattering techniques, the usual method for measuring the "droplet" sizes is by means of transmission electron microscopy and electron diffraction after cutting the cooled sample into thin foils (ref. 4,5). A typical example of such results, obtained by Speich and Oriani (ref. 29), for the growth of Cu-precipitates in Cu-Fe alloy is shown in Fig. 3. The same data are plotted against $t^{1/3}$ and

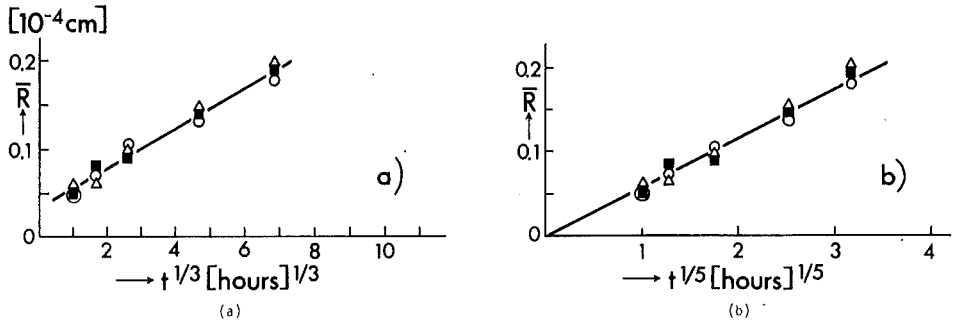

Fig. 3. Time evolution of the mean particle radius of Cu-precipitates in α-Fe. The same data are plotted versus $t^{1/3}$(a) and versus $t^{1/5}$ (b) (from ref. 29).

$t^{1/5}$, demonstrating that while the increases in the mean particle radius can be represented by a power law:

$$\bar{R} \sim t^{a'}, \tag{3}$$

where the exponent a' is a small number; the exponent cannot be determined unambiguously from this experiment. The Lifshitz-Slyozov theory (ref. 6) predicts a' = 1/3, but the data seem to be consistent with smaller values for a' as well. Results similar to those shown in Fig. 3 have been obtained by other authors on a variety of systems (ref. 4,5). The particle size distribution at late times was also determined in some cases from the data (ref. 5), although only crudely. We do not discuss these measurements in detail because most of them are rather imprecise. One further example, which seems to give a more convincing confirmation of the Lifshitz-Slyozov theory (ref. 6), is shown in Fig. 4. These results, taken from

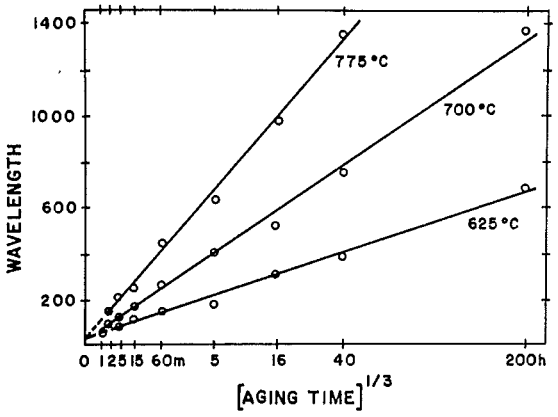

Fig. 4. Plot of the "characteristic wavelength" of the precipitated zones of a quenched Cu-N_i-Fe alloy versus (aging time)$^{1/3}$ for three temperatures (from ref. 30).

Butler and Thomas (ref. 30), refer to the decomposition of a 51.5% Cu - 33.5% Ni - 15% Fe alloy.

Other techniques used for studying quenched alloys include magnetic measurements (ref. 30) and measurements of the electrical resistivity (ref. 31). While these techniques have some distinct advantages, they yield only indirect information and hence their interpretation is rather difficult and we will not discuss them furhter.

In general, we may expect that in all experiments on real substances there will be a complicated inerplay of different processes which will make their theoretical interpretations difficult; e.g., a different behavior is obtained if the diffusion of atoms occurs preferentially on grain boundaries or dislocations (ref. 32), or if the reaction of the atoms with grain surfaces rather than diffusion in the matrix is the rate-determining step (ref. 33) for the coarsening. In addition, due to the difference in lattice spacing between the two constituents, long range elastic distortions build up which tend to destroy the matrix lattice, resulting in "loss of coherence" (ref. 30).

There are also problems which prevent the experimentalist from studying the very early stages of the process:

1. The clustering on the atomic length scale which occurs at the initial stages is beyond the resolution of usual electron micrograph techniques, and in x-ray or neutron scattering there are often problems with the intensity due to background, etc.

2. Complications arise from the effects of finite cooling velocity and resulting temperature gradients.

Thus, the interpretation of the available experiments is somewhat difficult, and the clarification provided by "computer experiments" on idealized simple model systems is needed.

ELEMENTARY DISCUSSION OF TEHORETICAL CONCEPTS

Classical theory

The macroscopic theory uses the concept of a coarse-grained concentration $\eta(\underline{r},t)$ which is a slowly varying function of $\underline{r}$, in contrast to $c(\underline{r},t)$ itself, which varies rapidly on a dimension of atomic scales (ref. 10). Such a theory in which rapid local thermal flucturations are averaged out should be a much simpler description of the processes in which we are interested here. A disadvantage of this approach is, of course, that it is hard to give a precise definition of $\eta(\underline{r},t)$. We may think of it, as is done in hydrodynamics, as the number of particles in a volume ω centered at $\underline{r}$ divided by the volume of ω, which volume is very small on a macroscopic scale but large enough to contain "many" molecules.

It is easiest to consider first the case where $\eta(\underline{r},t) = \bar{c}$ is uniform throughout the system. Now if $\bar{c}$ is is the one phase region of the system, then the true

equilibrium Helmholtz free energy of the system will be given by:

$$F(\bar{c}) = VF(\bar{c}) = \int_V d\underline{r}\, f(\bar{c}), \tag{4}$$

where V is the volume of the system (and we have omitted the dependence on the temperature). As already mentioned, the classical Cahn-Hilliard theory (as well as the theory of Langer and coworkers [ref. 10-12]) makes the assumption that it is possible to define a meaningful free energy for a system having a temperature T and average density $\bar{c}$ inside the coexistence curve which is <u>not</u> separated into two phases. Such a system is of course not in equilibrium and such a free energy can therefore not be derived form the standard formalism of statistical mechanics or of thermodynamics without further assumptions; see the article by Penrose and Lebowitz (ref. 19) and also Reiss (ref. 9). To avoid dealing with this problem, it is usually simply assumed that $f(\bar{c})$ can somehow be extended into the two-phase region and that the $F(\bar{c})$ corresponds either to a "local" minimum or to a local maximum in the free energy over all concentrations $\{n(\underline{r})\}$ which are "close" to the uniform density. The global minimum corresponds to a phase separation. (This analysis can actually be made rigorous for systems with very long range potentials, c.f., Penrose and Lebowitz [ref. 18,19].) The simplest function having this behavior, and which leads to the phase diagram of Fig. 1, is $f(\bar{c}) = \frac{1}{2}A(\bar{c} - c_{cr})^2 + \frac{1}{4}B(\bar{c} - c_{cr})^4 + f(c_{cr})$ with $A(T) < 0$ for $T < T_c$. The next assumtion which is made is that if $\Psi(\underline{r}) \equiv n(\underline{r}) - c_{cr}$ is not spatially uniform, then it is still possible to write a free energy functional which involves, in addition to Ψ, only its gradient $\nabla\Psi$, i.e.:

$$F = \int_V d\underline{r}\left(\tfrac{1}{2}A\Psi^2(\underline{r}) + \tfrac{1}{4}B\Psi^4(\underline{r}) + \tfrac{1}{2}K[\nabla\Psi(\underline{r})]^2\right) + F(c_{cr}), \tag{5}$$

where A, B and K can depend on T with $A(T) < 0$ for $T < T_c$ and B and K always positive. The integrand in Eq. 5 is interpreted as a "quasi" local free energy density.

The motivation for introducing the "free energy" defined by Eq. 5 is to obtain, by taking the (functional) derivative of F with respect to Ψ at position $\underline{r}$, taking into account the constraint of constant composition, an effective local chemical potential $\mu(\underline{r})$:

$$\mu(\underline{r}) = \frac{\delta F}{\delta\Psi(\underline{r})}\,. \tag{6}$$

(Actually, since we are dealing with a two-component system, F should be a functional of two coarse-grained concentrations, $\Psi_A(\underline{r})$ and $\Psi_B(\underline{r})$ with $\mu_\alpha(\underline{r}) = \delta F/\delta\Psi_\alpha(r)$, α = A,B. According to our assumption, however, the total coarse-grained density is fixed so that $\mu(\underline{r})$ should be interpreted as the difference, $\mu_A(\underline{r}) - \mu_B(\underline{r})$.) It is now assumed that the gradient of $\mu(\underline{r})$ will act as a driving force for a current

$\underline{J}$ (A atoms in one direction, B atoms in the opposite direction):

$$\underline{J} = -M\underline{\nabla}\,[\mu(\underline{r})] = -M\nabla[A\psi(\underline{r}) + B\psi^3(\underline{r}) - K\nabla^2\psi(\underline{r})], \tag{7}$$

where M is a diffusion constant (or mobility). This term will generally lead to a time variation in ψ. The equation describing the time evolution of $\psi(\underline{r},t)$ is obtained by combining Eq. 7 with the conservation of mass expressed by the continuity equation:

$$\frac{\partial\psi(\underline{r},t)}{\partial t} + \nabla J(\underline{r},t) = 0. \tag{8}$$

This procedure yields the basic equation of the Cahn-Hilliard theory:

$$\frac{\partial\psi(\underline{r},t)}{\partial t} = M\nabla^2[A\psi(\underline{r},t) + B\psi^3(\underline{r},t) - K\nabla^2\psi(\underline{r},t)]. \tag{9}$$

Let us first discuss the case where ψ is a constant so that $\underline{J} = 0$; i.e.,:

$$\mu = A\bar{\psi} + B\bar{\psi}^3. \tag{10}$$

It is seen that the minimum of F occurs when $\mu = 0$ (this is simply a matter of normalization) which putes the coexistence curve at:

$$\bar{\psi}_{coex} = \pm\sqrt{-A/B}\quad, \tag{11}$$

If we consider the response function ("susceptibility") χ defined by:

$$\chi^{-1} \equiv \frac{\partial\mu}{\partial\psi}\,,\ \chi^{-1} = A + 3B\bar{\psi}^2, \tag{12}$$

it is found that χ^{-1} vanishes (and changes sign) at a stability limit ("spinodal curve") given by:

$$\bar{\psi}_{spinodal} = \sqrt{-A/3B} \tag{13}$$

The crucial role played by the spinodal curve can be understood by considering the dynamics. To do so, we linearize Eq. 9 around $\bar{\psi}$ as determined by Eq. 10, i.e., we write:

$$\psi^3(\underline{r},t) = \{\bar{\psi} + [\psi(\underline{r},t) - \bar{\psi}]\}^3 \approx \bar{\psi}^3 + 3\bar{\psi}^2[\psi(\underline{r},t) - \bar{\psi}]. \tag{14}$$

Then we obtain from Eq. 9:

$$\frac{\partial \Psi(\underline{r},t)}{\partial t} = M\nabla^2 \left[(A + 3B\bar{\Psi}^2) - K\nabla^2\right] \Psi(\underline{r},t). \tag{15}$$

Eq. 15 can be solved by Fourier transformation. Setting:

$$\Psi(\underline{r},t) = \sum_{k} e^{ik\cdot r}\, \phi(\underline{k},t), \tag{16}$$

we obtain:

$$\frac{\partial \phi(\underline{k},t)}{\partial t} = -Mk^2 \left[(A + 3B\bar{\Psi}^2) + Kk^2\right] \phi(\underline{k},t). \tag{17}$$

The solution of Eq. 17 gives and exponential relaxation:

$$\phi(\underline{k},t) = \phi(\underline{k},\infty) + [\phi(\underline{k},0) - \phi(\underline{k},\infty)] \exp\{-Mk^2 t[(A + 3B\bar{\Psi}^2) + Kk^2]\}. \tag{18}$$

If the composition $\bar{\Psi}$ is outside the *spinodal* curve, we have $A + 3B\bar{\Psi}^2 > 0$ and the time constant of the exponential is positive for all small vectors k of the concentration fluctuations. This result means that the homogeneous state $\bar{\Psi}$ is stable with respect to any infinitesimally small fluctuation (where Eq. 14 is appropriate), i.e., we have a stable or metastable state. The former will of course occur outside the coexistence curve, while the latter corresponds to uniform systems with composition $\bar{c}$ between the coexistence and spinodal line. Since in both cases, however, the uniform state is a *stationary solution of Eq. 9* which is stable with respect to small perturbations, Eq. 9 predicts an infinite lifetime for the metastable state.

More interesting is the behavior within the spinodal curve where fluctuations increase exponentially with time, provided their wave vector k does not exceed a critical value k_c given by:

$$k_c = \sqrt{-(A + 3B\bar{\Psi}^2)/K}\ . \tag{19}$$

The maximum growth rate occurs at:

$$k_m = k_c/\sqrt{2}\ . \tag{20}$$

The enhancement of fluctuations within the spinodal means that the homogeneous state $\bar{\Psi}$ is unstable and phase separation sets in.

Theories including fluctuations

As mentioned already in the Introduction, some of the basic predictions of the classical theory, such as the sharp distinction between the behavior inside and

outside the spinodal region, are not in agreement with observations. This prediction of the theory is unfortunately not changed if we take a more general expression, $f(\Psi)$, for the local free energy function instead of the simple Landau expression, $\frac{1}{2}A\Psi^2 + \frac{1}{4}B\Psi^4$; it only leads to the replacement of the factor $A + 3B\bar{\Psi}^2$ by $(\partial^2 f/\partial\Psi^2)\bar{\Psi}$ in the determination of the spinodal region. It is neglect of intrinsic thermal fluctuations, those which have to be put in explicitly when one uses a macroscopic (course-grained) description of the physical system, which is responsible for the infinite lifetime of the metastable states in the region between the coexistence curve and the spinodal curve.

Among the first attempts to take fluctuations into account was the work of Cook (ref. 34) who obtained the following linear equation for the Fourier transform of the correlation $S(\underline{k},t)$ defined in Eq. 1:

$$\frac{\partial S(\underline{k},t)}{\partial t} = -2Mk^2 \{[(A + 3B\bar{\Psi}^2) + Kk^2]\, S(\underline{k},t) - k_B T\}, \tag{21}$$

with k_B = Boltzmann constant. (The extra factor of 2 in Eq. 21 as compared with Eq. 17 is essentially due to the relation $S(k,t) \propto |\phi(k,t)|^2$, and the extra $k_B T$ introduces thermal fluctuations.) This equation, which is indeed an improvement over Eq. 17, still, however, predicts a sharp transition at the spinodal line.

Furthermore, both Eqs. 17 and 21 predict that inside the spinodal region $S(\underline{k},t)$ increases exponentially for all k-values in the range $0 < k < k_c$, and develops a steadily increasing peak at the value k_m which is independent of time. Such behavior would imply that no particle coarsening occurs since the typical wavelength does not change with time. This fact is a consequence of the neglect of the nonlinearities in Eq. 14. (Langer [ref. 10] gave some arguments according to which the nonlinear terms should lead to a behavior $k_m(t) \propto t^{-1/3}$ in three dimensions.) Similarly, the unlimited exponential increase of fluctuations predicted by Eqs. 17 and 21 is actually limited by nonlinear terms in $\Psi(\underline{r},t)$ neglected in Eq. 14.

Thus, even if Eq. 9 was valid, Eqs. 15-21 would be expected to hold only for the early stages of the phase separation process. However, as we shall see later, the computer simulation results make it very doubtful that the linear theory is a valid description at all. This analysis casts doubt also on the validity of the nonlinear theory which, as emphasized already, has been derived in an entirely phenomonological manner.

To obtain a more microscopic theory, Langer (ref. 10) formulated a master equation for a probability distribution of the "concentration function" $\Psi(\underline{r})$ of the system, $P\{\Psi\}$. This equation may be written as:

$$\frac{\partial P\{\Psi\}}{\partial t} = -\int d\underline{r}\, \frac{\delta J(\underline{r})}{\delta \Psi(\underline{r})}\,, \tag{22}$$

where the "probability current" $J(\underline{r})$ is given by:

$$J(\underline{r}) = Mv^2 \left\{\frac{\partial f}{\partial \psi(\underline{r})} - K\nabla^2\psi(\underline{r}) + k_B T \frac{\delta}{\delta\psi(\underline{r})}\right\} P\{\psi\} \ . \qquad (23)$$

This approach still postulates the existence of a local free energy function, $f(\psi)$, but is more microscopic in that $\psi(\underline{r})$ is now considered as a "random" field with a certain probability distribution whose average value is the macroscopic concentration. If Eq. 22 is multiplied by $\psi(\underline{r})\ \psi(\underline{r}')$, integrates over the probability distribution P and again takes Fourier transforms, one obtains instead of Eq. 21 a similar equation:

$$\frac{\partial S(\underline{k},t)}{\partial t} = -2Mk^2 \{Kk^2 S(\underline{k},t) + \Omega(\underline{k},t) - k_B T\} \ , \qquad (24)$$

where the quantity $\left(\frac{\partial^2 f}{\partial^2 \psi}\right)_\psi S(\underline{k},t)$ in Eq. 21 is replaced by a function, $\Omega(\underline{k},t)$, which contains higher order correlation functions. Thus, Eq. 24 is not a closed equation, and in order to obtain a solution at all, it is necessary to approximate the term $\Omega(\underline{k},t)$ in some way.

The simplest approximation which goes beyond Eq. 21 is to make an assumption about the form of the probability distribution $P\{\psi\}$. Langer first assumed that $P\{\psi\}$ can be approximated by a Gaussian distribution centered at $\psi = 0$ (ref. 10, 35). This approximation leads, however, to a behavior similar to that described by Eq. 9. The unsatisfactory nature of this approximation can be understood from the fact that the actual $P\{\psi\}$ peaks at the two values of ψ corresponding to the concentrations on the coexistence curve c_A and c_B rather than having one peak at $\psi = 0$.

A substantially better approximation is obtained (ref. 12) if one approximates the two-point probability density $P_2\{\psi(\underline{r}),\ \psi(\underline{r}')\}$. Specifically, a closed equation for $S(\underline{k},t)$ is obtained if one writes:

$$P_2\{\psi(\underline{r}),\ \psi(\underline{r}')\} = P_1\{\psi(\underline{r})\}P_1\{\psi(\underline{r}')\}[1+\gamma(|\underline{r}-\underline{r}'|)][\psi(\underline{r}) - \bar{\psi}][\psi(\underline{r}') - \bar{\psi}]. \qquad (25)$$

Here, $P_j\{\psi(\underline{r}_1),\ldots,\psi(\underline{r}_j)\}$ is the probability density for finding specified values of the concentrations at positions, $\underline{r}_1,\ldots,\underline{r}_j$. The P_j will depend also on the time t and on the positions $\underline{r}_1,\ldots,\underline{r}_j$. Clearly, $\gamma = 0$ makes $\psi(r)$ and $\psi(r')$ statistically independent. Generally, $\gamma(|\underline{r}-\underline{r}'|)$ is related to the concentration correlation function (ref. 12):

$$\Omega(\underline{k},t) = S(\underline{k},t)\ A(t), \qquad (26)$$

where the function A(t), which is independependent of k, has to be determined self-consistently. The solutions of Eq. 24 can be obtained only numerically in

this case, and additional simplifying assumptions are necessary in order to obtain explicit results (ref. 12). Since it is not obvious how accurate these approximations (and the basic assumption of Eq. 25) are, it has to be stated again that computer simulation results are necessary as a check of the theory. Also, the validity of the coarse-graining procedure which gives Eq. 23 may be open to doubt in some cases.

Theories for the asymptotic time-dependence of the coarsening

In order to interpret the experiments, one wants also predictions for the rate at which the precipitated zones grow at large times. We have already mentioned the prediction of the (nonlinear) Ginzburg-Landau theory (ref. 10):

$$k_m(t) \sim t^{-1/3}. \tag{27}$$

Since the validity of this approach is rather uncertain, it is interesting to note that essentially the same result, Eq. 27, is obtained by a rather different approach using the linearized diffusion theory of Lifshitz and Slyozov (ref. 6).

One may summarize the main idea of this theory as follows (ref. 36). We consider a concentration $\bar{c}$ rather close to c_A and a very late stage of the coarsening. It should then be possible to describe the state of the system as a collection of (spherical) grains which have the composition of the B-branch of the coexistence curve c_B. Because of surface effects, these grains should not be in thermal equilibrium with a surrounding matrix having concentration c_A, but with one having a slightly enhanced concentration of B-particles given by:

$$c_R = c_A(1 + \frac{\text{const.}}{R}), \tag{28}$$

where R is the radius of the grain considered.

Eq. 28 is related to the well known expression for the formation energy of a droplet of a B-rich phase of concentration c_B from an A-rich phase of concentration $\bar{c}$. This expression has two terms: (1) a volume term, in which appears $\tilde{f}(c)$, the appropriate thermodynamic potential, and (2) a surface term containing the surface free energy F_s, Explicitly, in three dimensions:

$$\Delta F_R = \frac{4\pi R^3}{3} [\tilde{f}(c_B) - \tilde{f}(\bar{c})] + 4\pi F_s R^2. \tag{29}$$

In order that bulk phases (where the surface terms are negligible) shall coexist at concentration c_A and c_B, we must have:

$$\tilde{f}(c_A) = \tilde{f}(c_B).$$

Since we assumed that $\bar{c}$ is close to c_A, we may expand:

$$\tilde{f}(c_B) - \tilde{f}(\bar{c}) \cong \tilde{f}(c_B) - \tilde{f}(c_A) - (\bar{c} - c_A) \left.\frac{\partial \tilde{f}}{\partial c}\right|_{c_A} = - (\bar{c} - c_A) \left.\frac{\partial \tilde{f}}{\partial c}\right|_{c_A}. \tag{30}$$

Now Eq. 30 is used in Eq. 29 and we minimize the resulting expression for ΔF_R with respect to R in order to find the equilibrium radius at a given $\bar{c}$:

$$\frac{\partial \Delta F_R}{\partial R} = 0 = - 4\pi R^2 (\bar{c} - c_A) \left.\frac{\partial \tilde{f}}{\partial c}\right|_{c_A} + 8\pi F_s R,$$

and obtain $\bar{c}(R) \equiv c_B$ from this equation, which gives Eq. 28.

If we have a grain in whose surroundings the concentration is lower than that implied by Eq. 28, evaporation from the grain will outweigh the condensation. Similarly, condensation will dominate if the surrounding concentration is too high. When the criteria of Eq. 28 are satisfied, the grain, according to this analysis, will remain stationary, balanced by the two opposing tendencies. Note, however, that coarsening could stop at the *equilibrium* described by Eq. 28. According to Eq. 29, such a state would correspond to a maximum, rather than a minimum, in the free energy and so is unstable to fluctuations in either direction. There is, on the other hand, a certain stabilizing mechanism in that evaporation of a grain leads to an environment richer in B-particles and vice versa. Hence, to understand fully the kinetics of this process, we must therefore consider the global picture when there are grains of various sizes present in the system.

Consider now two neighboring grains a distance L apart of size R and $R + \Delta R$, respectively. Each grain has, when in "equilibrium", a different nearby B concentration given by Eq. 28. The difference between these values implies a concentration gradient between the surroundings of the two clusters of magnitude:

$$c_A \left[\frac{\Delta R}{R(R + \Delta R)}\right] \frac{1}{L} \quad . \tag{31}$$

The typical distance between grains is roughly linear in the average grain size $\bar{R}$ because the composition $\bar{c}$ is fixed. Assuming now that $R \approx \Delta R \approx \bar{R}$, we get concentration gradients $\propto 1/\bar{R}^2$. A diffusion current will result whose order of magnitude is:

$$J \propto M/\bar{R}^2, \tag{32}$$

which will destroy the unstable equilibrium for the isolated clusters. For a d-dimensional system (where all previous considerations still hold), the change of mass (or volume) $d(\bar{R}^d)/dt$ of a grain is then given by the total current through its surface (whose area is proportional to $\bar{R}^{d-1}$), i.e.:

$$\frac{d(\bar{R}^d)}{dt} \propto \bar{R}^{d-1} \quad J \propto M\bar{R}^{d-3}.$$

Hence,

$$\frac{d\bar{R}^3}{dt} \propto \text{const.}, \text{and } \bar{R}^3 = R_o^3 + \text{const. } t. \tag{33}$$

This linear relationship of $\bar{R}^3$, which corresponds to grain volume in three dimensions, with time is consistent with Eq. 27, as well as with other methods of analysis (ref. 6,36).

This simple argument, using equilibrium assumptions and macroscopic concepts (Eqs. 28,29), does not seem appropriate for intermediate times and intermediate grain sizes, even if it is appropraite for very late stages. Another coarsening law is obtained (ref. 7,36) by a more microscopic consideration of evaporation and condensation of the atoms from grains of radius R. A dimensional kind of justification may be used to make the new law plausible in the following way. First, note that the probability for the evaporation of B-atoms from a B-rich grain depends only upon the local geometric arrangement of atoms in the vicinity of this grain, and not on the concentration in the rest of the system. Then if a B-atom is evaporated, it performs a random walk in the A-phase region close to the surface of the grain. This random walk is otherwise unrestricted. An analysis of the properties of such random walks readily shows (ref. 36) that the probability that the atom diffuses up to a distance R from the grain without hitting the grain surface again decreases at least as strongly as 1/R. For large grains, the overwhelming majority of evaporated atoms rejoin the grain. By this process, the grain surface is rearranged, and the center of gravity of the grain is shifted a little. A large probability for recapture means a small probability of large excursions by the evaporated atom. Therefore, the mean distance (λ) between the site of evaporation and the site of reimpingement is usually only a few lattice spacings.

The shift of the center of gravity ($\underline{x}_G$) produced by such a process is given by (ref. 36):

$$\Delta\underline{x}_G \equiv \underline{x}_G' - \underline{x}_G = \Sigma_{\text{grain}}\, m(\underline{x}_i' - \underline{x}_i)/\Sigma_{\text{grain}}\, m = \lambda m/\sum_i m = \lambda'/R^d. \tag{34}$$

Here, we denote the mass of a B-atom by m and use the fact that the total mass of the grain is proportional to the grain volume; i.e., $\sum_i m \propto mR^d$ in d-dimensions, and λ' is a constant whose value is about 1, if lengths are measured in units of lattice spacings. If we measure the time in units where each atom has on the average one opportunity to be exchanged with one of its neighbors, we find for the rate of these processes in terms of a probability $p_{ev}(i)$ for evaporation of surface atom i:

$$\text{rate} = \sum_{\text{grain surface}} p_{ev}(i) = \bar{p}_{ev} \cdot S_R \propto \bar{p}_{ev} \cdot R^{d-1}. \tag{35}$$

In Eq. 35, we have made the further assumptions, reasonable for large clusters, that an average value of $p_{ev}(i)$, namely $\bar{p}_{ev}$, independent of R may be used for all clusters. Since we assume low temperatures here, where the grain is nearly pure B-phase, we also must have rather compact grains and hence a geometrical relationship $S_R \propto R^{d-1}$ holds. On that basis, we find for the cluster diffusion constant D_R, adding up the random displacement of its center of gravity as estimated in Eq. 34:

$$D_R \propto \text{rate } (\Delta \underset{\sim}{x}_G)^2 = \text{const } R^{d-1} (\lambda'/R^d) = \hat{D} R^{-1-d}. \tag{36}$$

The grains will coalesce if they come close enough to each other in their random walks. We next estimate the time Δt needed for a grain to diffuse across the mean distance $\propto \bar{R}$ between grains:

$$L^2 = D_{\bar{R}} \cdot \Delta t; \quad \Delta t \propto \bar{R}^2 / D_{\bar{R}} \propto \bar{R}^{3+d}, \tag{37}$$

and note that a change of volume of the order $\Delta R^d \approx (\bar{R})^d$ occurs when two grains coalesce. From:

$$\frac{\Delta \bar{R}^d}{\Delta t} \propto \frac{R^{-d}}{R^{3+d}} = \bar{R}^{-3}, \tag{38}$$

we find (ref. 7) immediately, putting $\Delta(R^d)/\Delta t = \partial(R^d)/\partial t$:

$$\frac{\partial \bar{R}}{\partial t} \propto \bar{R}^{-2-d}, \quad (\bar{R})^{3+d} \propto t, \quad \bar{R} \propto t^{1/(3+d)}, \tag{39}$$

which is a much smaller growth rate than the one predicted by Eqs. 37 and 33. If the latter predictions are correct, one would expect that the Lifshitz-Slyozov mechanism supersedes this cluster surface rearrangement and diffusion mechanism at long enough times. Again, of course, it is difficult to assess the validity of assumptions like Eq. 35, or even guess properly the magnitude of the constants not estimated here (ref 36) and hence computer simulations are necessary to decide whether a relaxation with the rate of Eq. 39 actually occurs.

SIMPLE MICROSCOPIC LATTICE MODELS OF BINARY ALLOYS

Equilibrium Properties

We consider a lattice where each site i may be occupied by either an A atom ($c_i^A = 1$, $c_i^B = 0$) or a B atom ($c_i^B = 1$, $c_i^A = 0$). We assume that the part of the Hamiltonian depending on these local concentration variables, c_i^A, c_i^B, can be represented by a sum of pair potentials and (local) chemical potentials $\mu_A(\underset{\sim}{r})$,

$\mu_B(\underline{r})$:

$$H = \sum_{i\neq j} [c_i^A\, c_j^A\, \varphi_{AA}(\underline{r}_{ij}) + 2c_i^A\, c_j^B\, \varphi_{AB}(\underline{r}_{ij}) + c_i^B\, c_j^B\, \varphi_{BB}(\underline{r}_{ij})] - \sum_i [c_i^A\, \mu_A(\underline{r}_i) + c_i^B\, \mu_B(\underline{r}_i)] + H_o. \tag{40}$$

The background term H_o contains the kinetic energy of the atoms. We assume a perfect lattice without vacancies, surfaces, etc., and then the pair potentials φ_{AA}, etc., depend only on the relative distance $\underline{r}_{ij} = \underline{r}_i - \underline{r}_j$ between the atoms. It is convenient to introduce a spin representation in terms of the variable $S_i = \pm 1$ using the relations:

$$c_i^A = (1 + S_i)/2,\ c_i^B = (1 - S_i)/2, \tag{41}$$

which leads to the Ising model Hamiltonian:

$$H = -\sum_{i\neq j} J(\underline{r}_{ij})\, S_i S_j - \sum_i H_i S_i + H_o = H_{Ising} + H_o', \tag{42}$$

where H_o' is a revised background including H_o and where the "exchange constant" J is given by:

$$2J(\underline{r}_{ij}) = \varphi_{AB}(\underline{r}_{ij}) - \tfrac{1}{2}[\varphi_{AA}(\underline{r}_{ij}) + \varphi_{BB}(\underline{r}_{ij})], \tag{43}$$

and the "magnetic field" H is given by:

$$2H_i = \sum_{j(\neq i)} [\varphi_{BB}(\underline{r}_{ij}) - \varphi_{AA}(\underline{r}_{ij})] + \mu_A(\underline{r}_i) - \mu_B(\underline{r}_i). \tag{44}$$

According to standard statistical mechanics, we may obtain the equilibrium properties of our system by calculating a partition function:

$$Z = \mathrm{Tr}\, \exp(-H/k_B'T). \tag{45}$$

Thermal averages of any quantity $Q(\{S_i\})$ are then given by:

$$\langle Q(\{S_i\})\rangle = \frac{1}{Z}\, \mathrm{Tr}\{\exp(-H/k_BT)\, Q(\{S_i\})\}. \tag{46}$$

We suppose now that $|J| \ll |\varphi_{AA}|, |\varphi_{BB}|$ and that $|\partial J/\partial \underline{r}_{ij}| \ll |\partial \varphi_{AA}/\partial \underline{r}_{ij}|, |\partial \varphi_{BB}/\partial \underline{r}_{ij}|$. Then the effect of the set of variables $\{S_i\}$ on the properties of the lattice (for example, the dependence of lattice spacing on temperature) may be neglected. In discussing the behavior of the $\{S_i\}$, we may replace $J(\underline{r}_{ij})$ by $J(\underline{x}_{ij})$, where

$\underline{x}_{ij}$ is the average distance between the particles belonging to lattice sites i, j, instead of their actual distance $\underline{r}_{ij}$ which may vary with time. We then approximate the average in Eq. 46, taken in a "compressible Ising lattice", by the much simpler average:

$$\langle Q\{S_i\}\rangle = \frac{1}{Z_{Ising}} \mathrm{Tr}\{\exp(-H_{Ising}/k_BT)\, Q(\{S_i\})\}. \tag{47}$$

This approximation is particularly bad if there is considerable "lattice misfit" between the two species A,B, since then elastic interactions (of long range) should be taken into account and this separation of variables is impossible. We thus assume that there is no lattice misfit, and in addition take $J(\underline{x}_{ij})$ to be nonzero only between nearest neighbors, so that Eq. 47 reduces to the standard Ising problem considered extensively in the literature (ref. 37). Then, $c_{cr} = 0.50$ and the corresponding phase diagram is shown in Fig. 5 for both two and three dimensions. For d = 2, the coexistence curve is given by the exact result of Yang (ref. 38), while for d = 3 it is based on Padé approximants (ref. 39). It is important to note that close to T_c the behavior of the coexistence curve is:

$$\bar{\Psi}_{coex} = \langle m^*\rangle \sim (1 - T/T_c)^{\beta},\ \beta = 1/8 (d = 2), \beta \simeq 5/16 (d = 3), \tag{48}$$

(m^* is the spontaneous magnetization) which is not described correctly by the

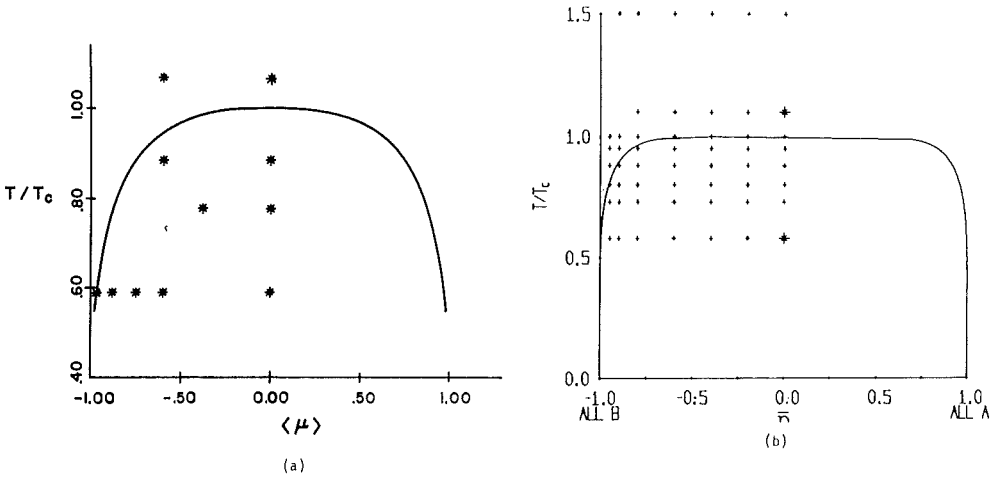

Fig. 5. Phase diagram of a three-dimensional (a) and a two-dimensional (b) Ising system. The points studied are indicated.

Landau theory of Section III, where $A = a(T - T_c)$ leads to $\beta = 1/2$ for both two and three dimensions. More important, one does not obtain any spinodal curve from equilibrium statistical mechanics (ref. 18,19). The spinodal curve as given in Eq. 13 is only an artifact of the approximation. One can therefore *hope* to obtain a meaninfgul spinodal curve only from nonequilibrium considerations, where it *could* separate regimes of different dynamic behavior (ref. 18,19,16). Its location or even its existence may depend on the dynamics of the processes considered. Numerical investigations of dynamic properties of two-diemnsional simple-spin-flip kinetic Ising models suggest that in this case the "spinodal" curve is not very sharply defined and is extremely close to the coexistence curve (ref. 17, 40,41). In three dimensions, the spinodal curve, if it can be defined at all, is probably much closer to the coexistence curve than Eqs. 11 and 13 would suggest (ref. 41).

Time-dependent properties

The Ising Hamiltonian defined in Eq. 42 does not have any dynamics of its own. Of course, the kinetic energy terms contained in H_0 and H_0' will also depend on the $\{S_i\}$ and thus provide a time evolution of the $\{S_i\}$. Since the $\{S_i\}$ evolve at a much slower time scale than do the thermal fluctuations of the lattice (lattice vibrations), one may treat the latter as a heat bath, which induces random exchanges between neighboring atoms. Since "memory effects" are only important on the time scale of the lattice vibrations, one may ignore them as far as the evolution of the $\{S_i\}$ is concerned, which is then described in terms of a Markovian master equation for the probability $P(S_1,\ldots,S_N,t) \equiv P(\underline{S},t)$.

The equation for $P(\underline{S},t)$ will contain a transition probability $W(\underline{S} \to \underline{S}')$, which gives the probability that the system makes a transition from a state $\underline{S}$ to a new state $\underline{S}'$. In fact, the transitions considered permit only the interchange of some S_i with a neighboring S_j so that $\{S_1', S_2', \ldots, S_i', \ldots, S_j', \ldots S_N'\} = \{S_1, S_2, \ldots, S_j, \ldots, S_i, \ldots, S_N\}$ for some neighboring sites i,j. The master equation then reads:

$$\frac{d}{dt} P(\underline{S},t) = -P(\underline{S},t) \sum_{S'} W(S' \to S) + \sum_{S'} W(\underline{S}' \to S)\, P(\underline{S}'). \tag{49}$$

Eq. 49 has the structure of a rate equation: the first term on the right hand side describes the decrease of the probability of configuration $\underline{S}$ due to all possible exchange processes; the second term describes the inverse reactions, which increase the chance of observing state $\underline{S}$.

When the system is in equilibrium at the temperature T, it will have the probability distribution $P_0(\underline{S}) = Z^{-1} \exp(-H/k_B T)$ (where we have dropped the subscript I) $P_0(\underline{S})$ should therefore be a stationary solution of Eq. 49, which will be automatically true if we impose a detailed balance condition on the transition

probability:

$$W(\underline{S}\rightarrow\underline{S}')\ P_o(\underline{S}) = W(\underline{S}'\rightarrow\underline{S})\ P_o(\underline{S}'), \tag{50}$$

which can be written in the alternative form:

$$\frac{W(\underline{S}\rightarrow\underline{S}')}{W(\underline{S}'\rightarrow\underline{S})} = \exp(-\delta H/k_B T), \tag{51}$$

where δH is the change in energy produced by exchange $\underline{S}\rightarrow\underline{S}'$. Of course, Eq. 51 does not specify $W(\underline{S}\rightarrow S')$ uniquely; but a simple choice consistent with Eq. 51 is:

$$W(\underline{S}\rightarrow\underline{S}') = \frac{1}{\tau}\ \frac{\exp(-\delta H/k_B T)}{1+\exp(-\delta H/k_B T)} = \frac{1}{2\tau}\ [1 - \tanh(\delta H/2k_B T)]. \tag{52}$$

The arbitrary time constant τ is taken to fit our time scale. In principle, τ could be calculated considering the thermally activated diffusion process of an A-atom in a B-lattice and vice versa, but this possibility is not considered here.

In the process described by Fig. 1, the steady state equilibrium distribution $P_o(S_1,\ldots,S_N)$ will be obtained only asymptotically for $t\rightarrow\infty$, and we will thus be interested in the time-dependent averages:

$$\langle Q(t)\rangle = \sum_{\{S_i\}} P(S_1,\ldots,S_N,t)\ Q(\{S_i\}). \tag{53}$$

To obtain the structure function $S(\underline{k},t)$, defined in Eq. 1, we have to put:

$$Q(\{S_i\}) = \frac{1}{N}\sum_{\underline{r},\underline{r}_1} e^{i\underline{k}\cdot\underline{r}}\,[S(\underline{r}_1) - \langle S\rangle]\ [S(\underline{r}_1+\underline{r}) - \langle S\rangle],$$

where $\langle S\rangle$ is related by Eq. 41 to the constant average concentration of B-atoms. From this definition, we note that:

$$\frac{1}{N}\sum_{\underline{k}} S(\underline{k},t) = 1 - \langle S\rangle^2,\ S(\underline{k}=0,t) = 0. \tag{54}$$

The physical interpretation of the latter relation is simply that there is no fluctuation of the average concentration during the evolution of our system.

It is interesting to note that the Cahn-Hilliard theory (ref. 1-3) can be derived (ref. 14) from our model by making certain mean field type approximations. This agreement is seen by putting $Q = S_i$ in Eq. 53, differentiating with respect to t and using Eqs. 42, 49 and 52. On the right hand side of the resulting equation, higher-order correlation functions are obtained. But replacing the expression:

$$\sum_{j(\neq i)} J_{ij} S_j \text{ by } \sum_{j(\neq i)} J_{ij} \langle S_j(t)\rangle$$

(i.e., neglecting fluctuations), one obtains a nonlinear equation for $\langle S_i(t)\rangle$ which no longer contains any higher order correlations functions. Making an expansion:

$$\langle S_j(t)\rangle = \langle S_i(t)\rangle + (\underline{r}_j - \underline{r}_i)\cdot\nabla\langle S_i(t)\rangle + \tfrac{1}{2}[(\underline{r}_j - \underline{r}_i)\cdot\nabla]^2\langle S_i(t)\rangle + \ldots,$$

and putting $\tanh x \approx x - x^3/3$, one obtains precisely Eq. 9, since we may then identify $\psi(\underline{r},t)$ with $\langle S_i(t)\rangle$. This derivation (for details, see [ref. 14]) relates the phenomenological constants of the Cahn-Hilliard equation (Eq. 9) to microscopic interaction parameters and elucidates the basic approximation, namely, the neglect of fluctuations. The advantage of our stochastic model is, of course, that its numerical solution by the Monte Carlo method does not involve such approximations, and hence a sensitive test of the validity of such approximations can be obtained.

In order to discuss the theories of grain growth (ref. 4-7,36) within the context of our model, it is useful to introduce the definition of a "cluster": A cluster (ℓ,α) is a group of ℓ B-atoms, each of which has as a nearest neighbor at least one other B-atom of this cluster, and none of which has a nearest neighbor any B-atom outside of the cluster. α is used to denote symbolically properties of the cluster other than its size ℓ, e.g., its surface area. This definition provides a unique prescription for assigning to which cluster any B-atom belongs. (If $\bar{c} > 0.5$, it is useful to replace A and B in this definition.) One may then proceed to define quantitites like the average cluster concentration, $\bar{n}_\ell(t)$, of clusters of size ℓ, defined by $\bar{n}_\ell(t) = \frac{1}{N}\sum_\alpha N_\ell^\alpha(t)$, where $N_\ell^\alpha(t)$ is the total number of clusters (ℓ, α) in the system at time t. It seems reasonable to identify large clusters (at least when they are "compact") with the grains considered in nucleation theory (ref. 4-7,36).

COMPUTER SIMULATION OF TIME EVOLUTION

Description of the method

In the computer simulation one chooses a system size N and, using Monte Carlo techniques (ref. 42), explicitly carries out the Markov process described by Eqs. 49 and 52. The first step is to generate a starting configuration of the system. If the initial temperature (T') is taken very high ($T' \to \infty$), one may use a random spin configuration which is easily generated. To consider a finit initial temperature T', one would have to let the system evolve from the random starting configuration (using ordinary spin-flip Monte Carlo sampling [ref. 42,40,49]) until "thermal equilibrium" is reached for the temperature T! The configuration of the system in this thermal equilibrium state may then be used as a starting configuration for the spin-exchange procedure by which Eq. 49 is realized.

Having generated a starting configuration, a selection is made (again at random) of the coordinates of two neighboring lattice sites i,j, which shall be considered for an interchange. The energy change which would result from an interchange of these atoms is now calculated, using Eq. 42. Thus, one computes the transition probability W from Eq. 52 with $\tau = 1$, thus measuring times in units of "one Monte Carlo step/spin". Again a pseudo-random number ζ is chosen; the interchange of the spins is actually performed only if $W > \zeta$, otherwise the old configuration is retained. This process is repeated a large number of times. At suitable time steps, t, one records the value of the function $Q(\{S_i^{(t)}\})$ in the state $\{\underline{S}^t\}$ obtained by this procedure at the time step t. When this procedure is repeated "many" times with different initial configurations, then the average of the value $Q(\{S_i^t\})$ corresponds to the ensemble average $\langle Q(t) \rangle$ in Eq. 55. This procedure would constitute an exact realization of a discrete time master equation analogous to Eq. 49.

The size N in the computer simulations is dictated by a competition between the desire to make the system as large as possible so it imitates a macroscopic system and also reduces the number of different runs needed for averaging and practical computational considerations. The actual computer experiments have been made for square lattices with $N = 55 \times 55$ (ref. 14), 80×80 (ref. 23,14) and $N = 200 \times 200$ (ref. 26) sites in two dimensions, and $N = 30 \times 30 \times 30$, $50 \times 50 \times 50$ in three dimensions (ref. 25). Periodic boundary conditions are used in order to avoid edge effects due to "free surfaces". Nevertheless, one has to worry about possible finite size effects which could affect the results. If one deals with one-phase equilibrium states, finite size effects become important if the linear dimension of the system has the same order of magnitude as the correlation length of fluctuations (ref. 37,45,46). One may in fact obtain reasonably accurate estimates of the thermal equilibrium properties of infinite systems from Monte Carlo calculations on finite systems, apart from a temperature region of a few percent around the critical point T_c if one uses values of N like those mentioned above (ref. 46). The vicinity of T_c is hardly accessible due to the fact that there also occurs a "critical slowing down", and hence very large amounts of computing time would be required (ref. 42,46).

In a study of phase separation kinetics, finite size problems may occur even far from T_c. One such effect is due to the fact that the final thermal equilibrium state is one of two-phase equilibrium, and we thus get a contribution from the interface between the two phases. The relative magnitude of this contribution to the energy of the final state is of the same order as the inverse linear dimension $\left(N^{-1/d}\right)$ of the system. The coefficient of the $N^{-1/d}$ term can, however, be quite large and it is therefore necessary to try and correct for these interface effects (ref. 14-26).

In addition, it is difficult to study the very late stages of $S(\underline{k},t)$, since

the peak of this function shifts to very low values of k. Due to the finite size of N, one may compute $S(\underline{k},t)$ at discrete values only:

$$\underline{k} = \frac{2\pi}{N^{\frac{1}{2}}} (\rho_x,\rho_y) \quad [d = 2]; \quad \underline{k} = \frac{2\pi}{N^{1/3}} (\rho_x,\rho_y,\rho_z) \quad [d = 3], \tag{55}$$

where the ρ_x, ρ_y, ρ_z are integers. Therefore, in the case of d = 2, studies were made for both $N^{\frac{1}{2}} = 80$ and $N^{\frac{1}{2}} = 200$, and it was shown that this discreteness of momentum space did not appreciably affect the results (ref. 24,26).

A further effect related to the finite size of the system is the statistical inaccuracy; e.g., one expects statistical fluctuations in the energy of the system whose relative order of magnitude is $1/\sqrt{N}$. Furthermore, the starting configuration may not be a "typical" configuration at the temperature T! The starting statistical accuracy was tested making 8 runs with independent starting configurations, under otherwise identical conditions (ref. 24-26). Taking averages over these independent runs, the values of $S(\underline{k},t)$ to be presented below were obtained. The relative accuracy is believed to be better than 1% in the case of the energy and better than 20% in the case of $S(\underline{k},t)$.

It should be remarked that in the practical realization of computer experiments, limited computer time is often the most serious limitation, and hence it is important to devise a program which is as effective as possible (ref. 24-26). Thus, with nearest neighbor interactions an exchange may result in one of a few distinct values of δH (and hence W) only. Therefore, the possible values of W are computed before the calculation and stored in an array, instead of recomputing them over and over in the course of the procedure. It is also desirable not to select arbitrary pairs of neighboring spins for an exchange, but only those which consist of unlike spins (otherwise their exchange would not produce any change in the state of the system whatsoever!). Since the number of such pairs is not a constant during the time evolution of the system, one has to correct the relation between the "number of attempted exchanges" and the actual time appropriately. Nevertheless, the computations are very time consuming, since in the later stages of the segregation process most attempted exchanges lead to a $\delta H > 0$ and this W is quite small. Hence, many attempted exchanges are necessary until one actual exchange takes place. A further improvement of the algorithm which takes care of this problem (ref. 44) is expected to be useful in future computations of this type.

Finally, we remark that in order to obtain the quoted accuracy for $S(\underline{k},t)$ it was necessary to take "circular averages". That is, one takes averages over all (ρ_x,ρ_y) or (ρ_x,ρ_y,ρ_z) having the same magnitude:

$$\rho = \sqrt{\rho_x^2 + \rho_y^2} \quad (\text{or } \rho = \sqrt{\rho_x^2 + \rho_y^2 + \rho_z^2}, \text{ respectively}),$$

to the nearest integer:

$$S(k,t) = \sum_{k}' S(\underline{k},t)/\sum_{k}' 1, \qquad (56)$$

where the sum $\sum_{k}'$ goes over all values of (ρ_x,ρ_y) [or (ρ_x,ρ_y,ρ_z), respectively], such that $2\pi\rho \leq |\underline{k}|\ N^{1/d} < 2\pi(\rho+1)$. Since there is little physical interest in the behavior of S(k,t) at large k, S(k,t) was computed only for the 10 to 15 smallest values of k obtained in this way (depending on the value of N).

Results

Here we discuss mainly the results of Ref. 24,25,26; the much more restricted data of Ref. 23 are consistent with these results. We first examine the behavior of S(k,t) and then discuss the late time behavior of the energy and the grain size distribution.

Fig. 6 shows the initial time dependence of S(k,t) for a three-dimensional Ising alloy with composition $\bar{c} = 0.5$, quenched to $T = 0.6\ T_c$. Note that the critical tempeature T_c is related to the nearest neighbor "exchange constant" J via $k_B T_c \simeq 4.51\ J$ (ref. 37).

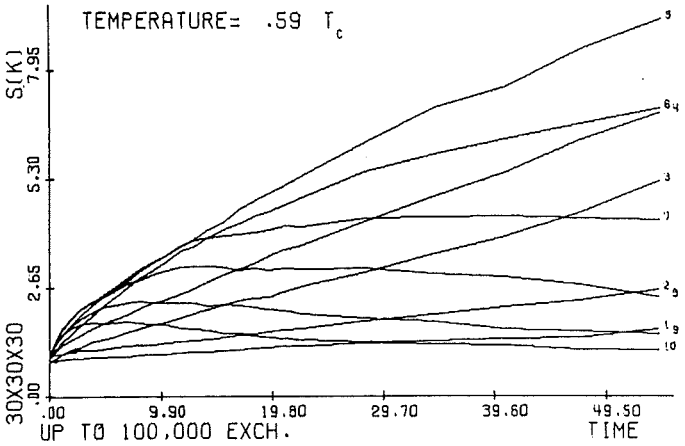

Fig. 6. Early-time evolution of S(k,t) as a function of time for different values of k for a three-dimensional alloy of composition 50% A; 50% B, quenched at $T = 0.6\ T_c$. At the end of each line is shown the corresponding value of $\rho = 30k/2\pi$ (from ref. 25).

According to the Cahn-Hilliard theory (ref. 1-3), these curves should be simple exponential functions, increasing with time for $k < k_c$ and decreasing with time for $k > k_c$ (c.f. Eqs. 18-21 and the subsequent discussion). Basically, the same prediction was obtained by more sophisticated theories for early stages of the time evolution (ref. 10,11). Fig. 6 is in remarkable disagreement with all of these predictions. Instead of an exponential increase with time, the increase is even weaker than linear with time! Only in the most recent versions of the

theory by Langer and coworkers (ref. 12), which was partially influenced by these results, could a description be obtained which is consistent with these numerical results.

In addition to the lack of any region of exponential increase, it is remarkable to observe that the curves reach a maximum and then decrease again. This behavior is even more pronounced if one considers the later stages of this process. It can be understood from the fact that the peak of the S(k,t) versus k-curves (Fig. 7) shifts to smaller values of k as time increases. While these curves are not

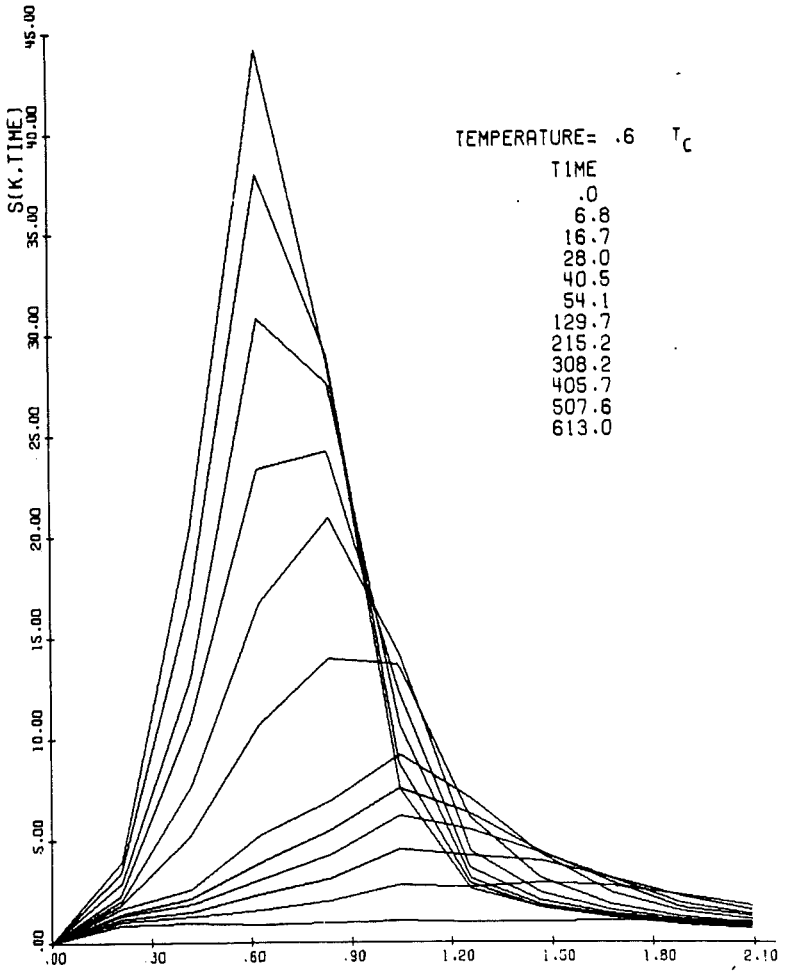

Fig. 7. Development with time of the spherical averaged structure frunction versus k for the system of Fig. 6. The increasing values of the time listed in the figure correspond to the different graphs from the bottom of the picture to the top. Note that the numerical results for S(k,t) at the available discrete values of k were connected by straight lines in between (from ref. 25).

at all in accord with the standard theories (ref. 1-3), their similarity to the experimental results (Fig. 2) is very striking.

It should be noted that the results for other temperatures are completely analogous as seen from Figs. 8 and 9, where data at $T = 0.9\ T_c$ are presented. Due to critical

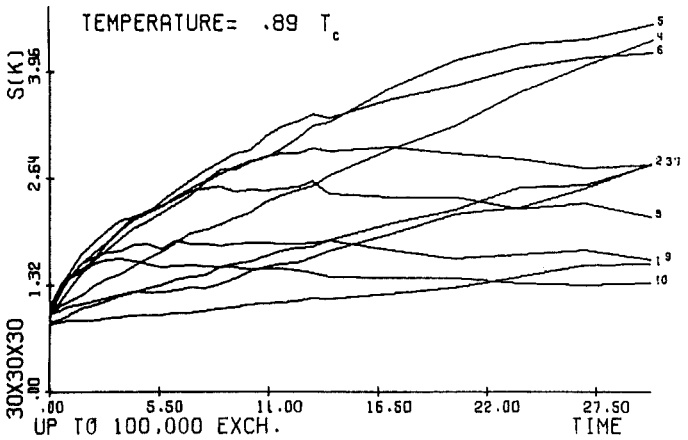

Fig. 8. Early time evolution of S(k,t) as a function of time, as in Fig. 6, but for $T = 0.9\ T_c$ (from Ref. 25).

slowing down, it now takes somewhat longer until the same peak heights of S(k,t) are reached. The results also look very similar if one chooses a lower concentration of B-atoms ($\bar{c} = 0.2$), as is done in Figs. 10-13. The only difference is that now S(k,t) does not decrease with time after reaching a maximum as in Figs. 6 and 8 for the chosen values of k, but rather stays constant. This behavior corresponds to the common "envelope" of all curves in Figs. 11 or 13 for larger values of k. Apart from this difference, which is in accord with the most recent theory (ref. 12), there is no pronounced dependence on concentration. On the contrary, the relaxation proceeds very similarly throughout the whole two-phase region. Therefore, the present results give little indication that one can find a well defined spinodal curve where the kinetic behavior changes drastically. This fact was tested more thoroughly in two dimensions, where a large number of compositions and temperatures were investigated (ref. 24-26) (see Fig. 5b). Here we show only a few selected examples at $\bar{c} = 0.5$ (Figs. 14,15) in order to demonstrate that the general features of the behavior are quite similar to the three-dimensional case.

In order to discuss the late-time behavior of $S(\underline{k},t)$ in terms of the power law predictions for the position of the maximum (ref. 6,7,36) [$k_m(t) \sim t^{-a'}$ of Eqs. 3, 27 and 39], we determined the first moment of S(k,t):

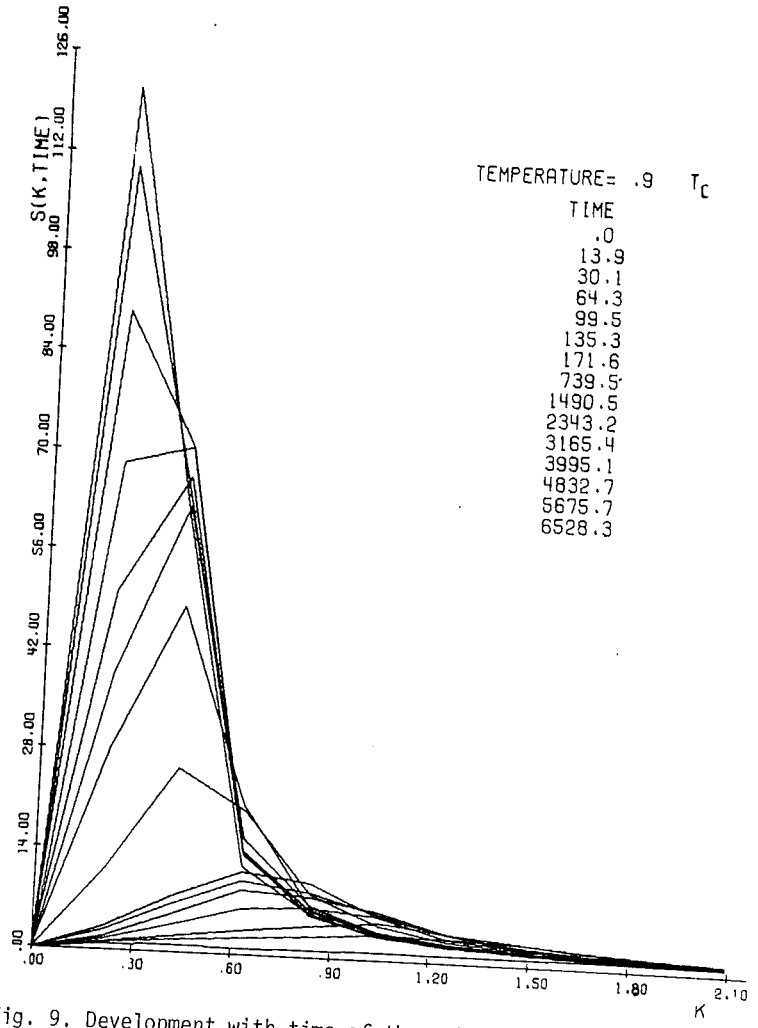

Fig. 9. Development with time of the spherical averaged structure function versus k for the system of Fig. 8 (from ref. 25).

$$\langle k_m(t)\rangle \equiv \frac{\sum_k kS(k,t)}{\sum_k S(k,t)} \quad . \tag{57}$$

An example is given in Fig. 16, where a log-log plot of $\langle k_m(t)\rangle$ vs. t is given. Power law behavior should show up as straight lines. The curvature of the graphs obtained does not allow any interpretation in terms of simple power laws, however. But one may interpret the data in terms of a crossover from power laws where the "cluster diffusion and cluster surface rearrangement" mechanism is valid (i.e., $a' = 1/6$ in three dimensions; cf. Eq. 39) to power laws with the quicker "cluster

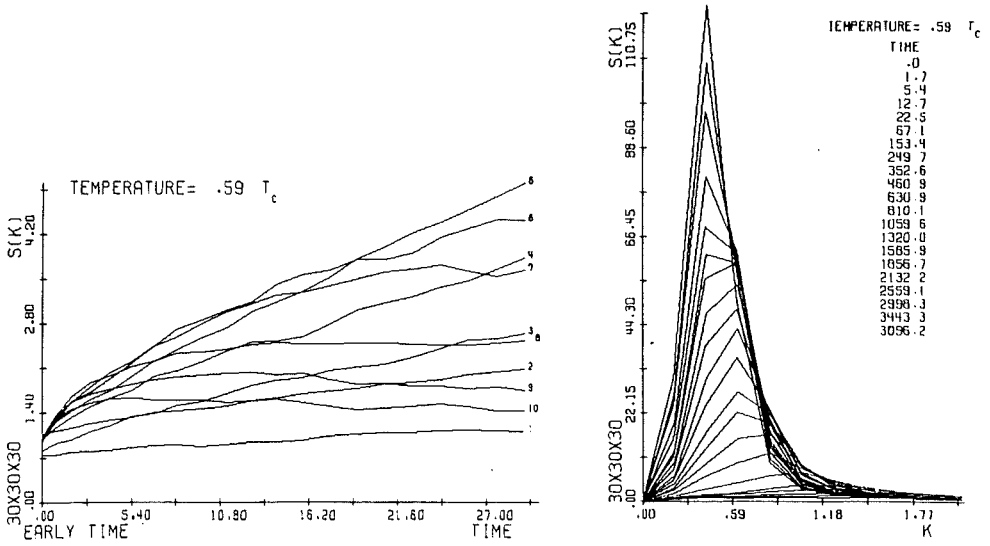

Fig. 10. Early time evolution of S(k,t) as a function of time for different values of k for a three-dimensional alloy of composition 80% A; 20% B, quenched at $T = 0.6\ T_c$. The corresponding value of $\rho = 30k/2\pi$ is shown at the end of each line (from ref. 25).

Fig. 11. Development with time of the spherical averaged structure function versus k of the system of Fig. 10 (c.f. Fig. 7 for explanations) (from ref. 25).

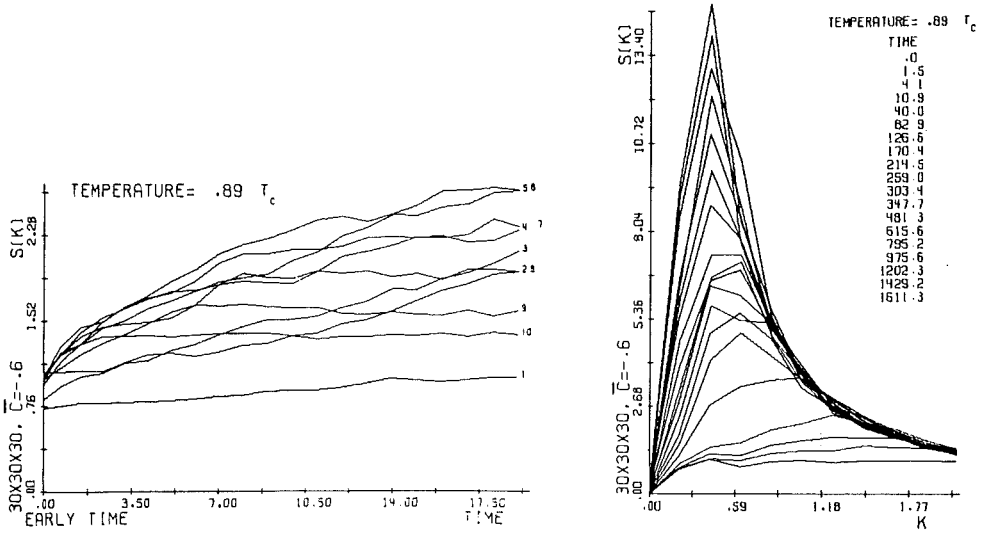

Fig. 12. Same plot as in Fig. 10, but for $T = 0.9\ T_c$ (from ref. 25).

Fig. 13. Same plot as in Fig. 11, but for $T = 0.9\ T_c$ (from ref. 25).

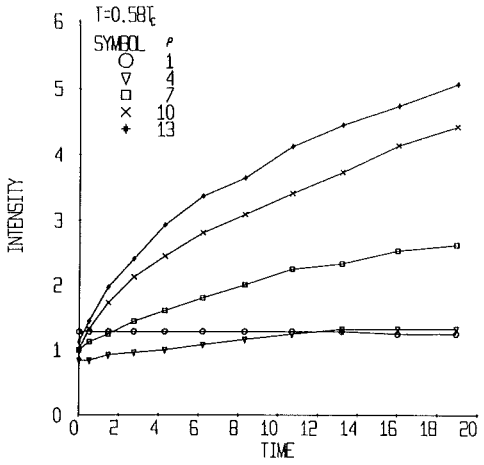

Fig. 14. Early growth of the structure function for representative k values (the numbers in the figure give the corresponding values of ρ) for a two-dimensional system of composition 50% A; 50% B, quenched at $T = 0.58\ T_c$ (from ref. 24).

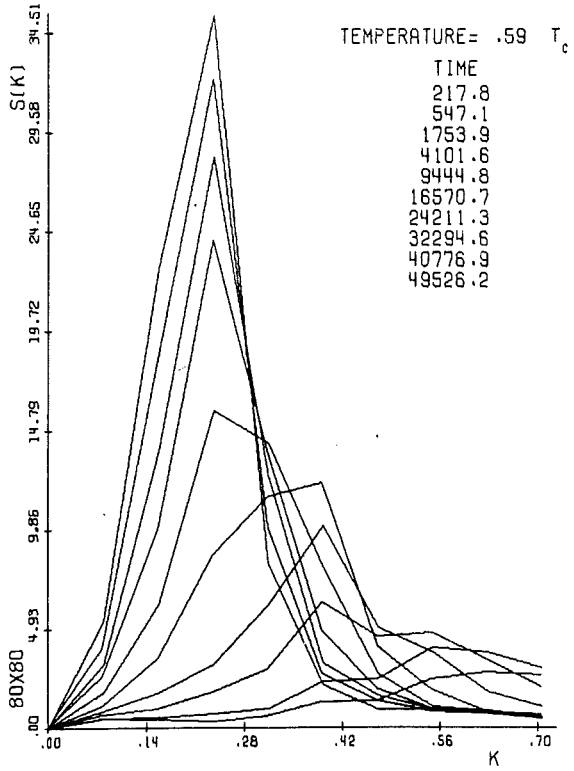

Fig. 15. Later-time development of the structure function in the two-phase region, the system being the same as in Fig. 14 (from ref. 26).

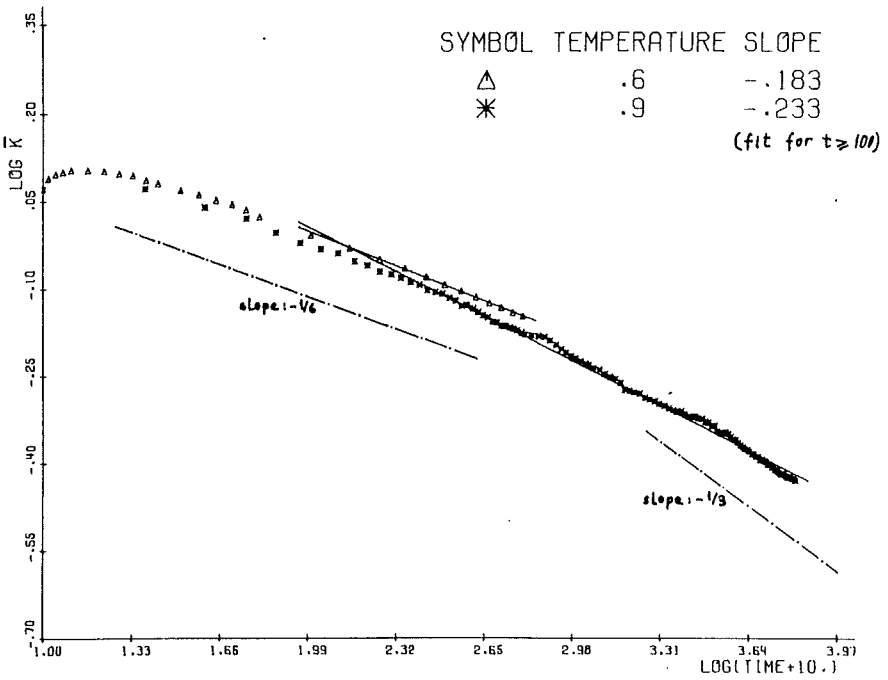

Fig. 16. Logarithm of the first moment of the structure function (Eq. 57) plotted versus the logarithm of the time for three-dimensional systems of 50% A; 50% B composition and several temperatures. The additive constant (10.) in the time scale was used to incorporate also the initial stages at this plot; it should be irrelevant for the determination of the asymptotic power law behavior (from ref. 25).

evaporation and condensation" mechanism (i.e., $a' = 1/3$, cf. Eq. 33), which should dominate at large enough times. This interpretation is, of course, somewhat speculative.

On the other hand, the results are in good numerical agreement with the results of Langer, Bar-On and Miller (ref. 12) in the range of time studies. This good agreement may be considered as a justification of the approximations that they made. A more detailed comparison with their predictions will be given later. Their work does not contain any explicit prediction for the asymptotic time dependence since it yields numerical results only. It can be argued (ref. 36), however, that for very late times the equations of Langer, Bar-On and Miller should yield $a' \simeq \frac{1}{4}$. If this assumption is correct, their treatment would seem to be inappropriate for the late times.

In order to clarify these questions converning the asymptotic power lawas, the time dependence of the excess energy $\Delta u(t) = u(t) - u(\infty)$ has also been recorded, where:

$$u = N_{AB}/N = q/2d + (1/2JN) \langle H \rangle. \tag{58}$$

Here, N_{AB} denotes the number of AB-nearest neighbor pairs in the lattice, and q is the coordination number. While u cannot be measured experimentally, it can be recorded very easily in the computer experiment and compared to the theoretical predictions (ref. 7,36), which imply:

$$\Delta u(t) \sim t^{-a'}. \tag{59}$$

The computer simulation results (see Fig. 17) seem to indicate again that two

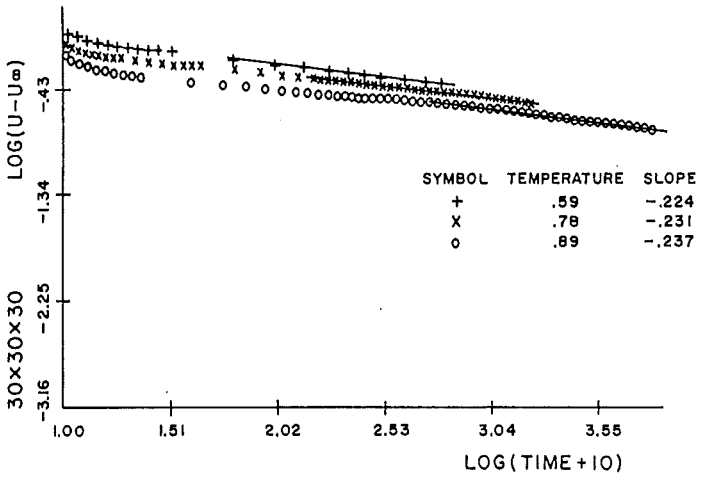

Fig. 17. Log-log plot of the excess energy versus time. The system studied is a three-dimensional simple cubic lattice with composition 50% A; 50% B, quenched at temperatures $T = 0.6\ T_c$m $0.8\ T_c$ and $0.9\ T_c$ (from ref. 25).

regimes with different behaviors have to be distinguished. For very long times, the results seem to be consistent with the Lifshitz-Slyozov (ref. 6) 1/3 law. A more definite conclusion is unfortunately not possible since there is considerable uncertainty concerning the correct values of $u(\infty)$ (ref. 25).

In order to facilitate a comparison with the theories on grain growth, the grains (or clusters) which form in the course of the relaxation process have been investigated directly. Of course, well separated grains occur at small enough concentrations only; at higher concentrations one rather obtains a percolating network (ref. 23). The following results refer to $\bar{c} = 0.2$, where well defined clusters were found both in two and three dimensions. It is interesting to note, however, that the late time behavior of S(k,t), $\Delta u(t)$, etc., seems to be unaffected by this percolation threshold.

In three dimensions, the quenched system goes rather quickly to a state where nearly all B-atoms belong to a few very large grains. Fig. 18 shows a "snapshot

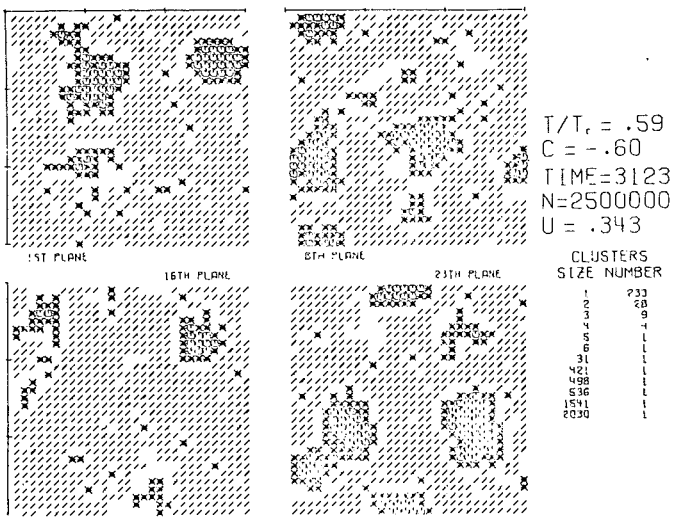

Fig. 18. Four cross sections of the 30 x 30 x 30 system with composition c = 0.2 quenched down to T = 0.6 T_c at time t = 3123 after the quench. The distance between these parallel planes is 8 atomic layers. The corresponding cluster distribution is also shown (from ref. 25).

picture" of four 30 x 30 planes of the system. Note that even rather large grains have still quite irregular shapes. Fig. 19 gives a plot of the mean grain size versus time. This result can be compared to the corresponsing experimental observations (Figs. 3 and 4). For the range of times studied here, the grain volume

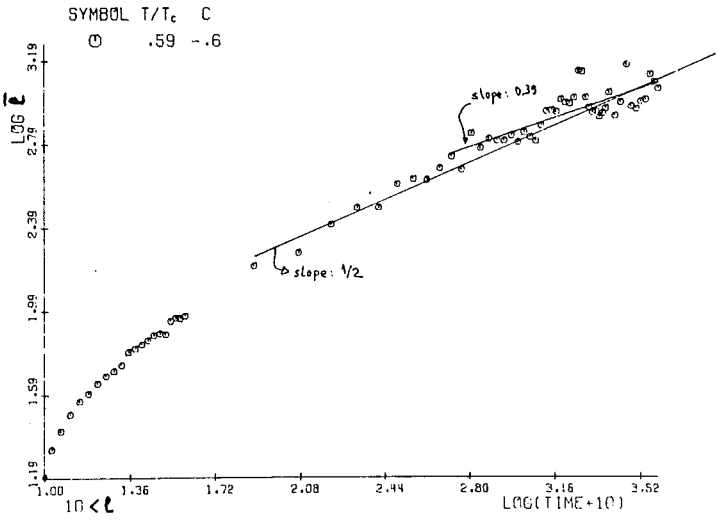

Fig. 19. Log-log plot of mean grain volume versus time for a three-dimensional lattice of composition c = 0.2 quenched at T = 0.6 T_c (from ref. 25).

does not yet follow the $V \sim t$ law (ref. 6) (Eq. 33). It must be noted, however, that the very smallest particle sizes observed experimentally correspond to the very largest ones observed in the computer experiment, and that visual inspection of different cross sections in the system (as those shown in Fig. 18) does not reveal the anomalous (very far from spherical) cluster shape which might also be characteristic of real quenched alloys.

We give more extensive results on the evolution of the cluster pattern in two dimensions, where observation is much easier. Figs. 20-23 show the evolution of a 200 x 200 system, quenched at $T = 0.59\ T_c$. The most striking difference with the three-dimensional case is that the clusters stay rather small during the whole course of observation. It is seen that the clusters become more compact as time goes on. Some small clusters evaporate while others coalesce or split into parts again. From the direct observation of all these processes, it can be said that the physical mechanisms postulated by the theories (ref. 6,7,36) described in the section entitled "Discussion of theoretical concepts - Theories for the asymptotic time-dependence of the coarsening" are certainly present. Unfortunately, there does not appear to be a well defined succession of various stages when different mechanisms are dominant, rather we observe all processes at the same time. This finding indicates that it will be necessary to incorporate their interplay into a quantitative theory.

Figs. 20-23 show that the kinetics of spinodal decomposition can, at least in principle, be described in terms of cluster formation and growth, as in nucleation theory. It is always the limitations due to the diffusion of atoms and the conservation of mass which determine the rate of growth. Again, the conclusion is that the kinetic behavior changes very gradually if one varies the composition, and one should not see any drastic change at a spinodal curve (ref. 48).

The grain size distribution is usually recorded in the experiments (ref. 4,5), and thus the evolution of the cluster size distribution with time has also been obtained (Figs. 24-27). These figures show that the system does not evolve toward a distribution of rather uniform grain size. The grain size spectrum stays very broad while its center shifts to larger values as time goes on. The large statistical fluctuations prevent us from making statements concerning the functional form of this distribution function. In Fig. 28 we give the time dependence of the mean cluster size in order to chekc the power law predictions of Refs. 6 and 7. Within the rather restricted regimes of time and grain sizes studied, the data are roughly consistent with the Binder-Stauffer predictions (ref. 7) but inconsistent with the Lifshitz-Slyozov theory (ref. 6).

Figs. 29 and 30 finally show snapshot pictures of an 80 x 80 lattice with equiatomic composition ($\bar{c} = 0.5$). Here, well separated clusters can no longer be distinguished. The resulting network of B-phase on the background of A-phase (or vice versa!) is quite irregular. The spinodal decomposition does not lead to any

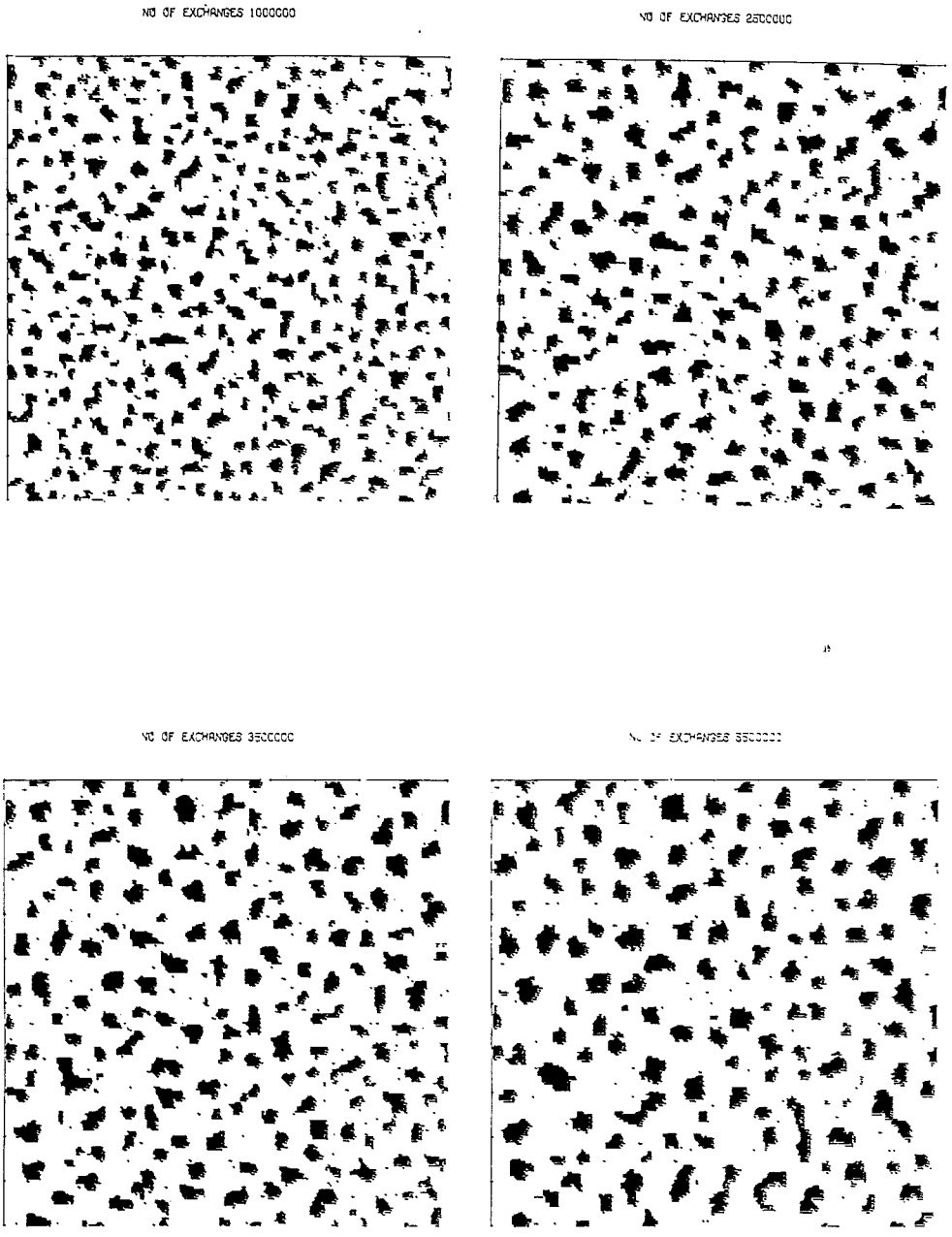

Figs. 20-23. "Snapshot pictures" of the configuration of a 200 x 200 system with composition c = 0.2 at various times after the quench to $T = 0.59\ T_c$. B-atoms are indicated as black dots, A-atoms are not shown (from ref. 26).

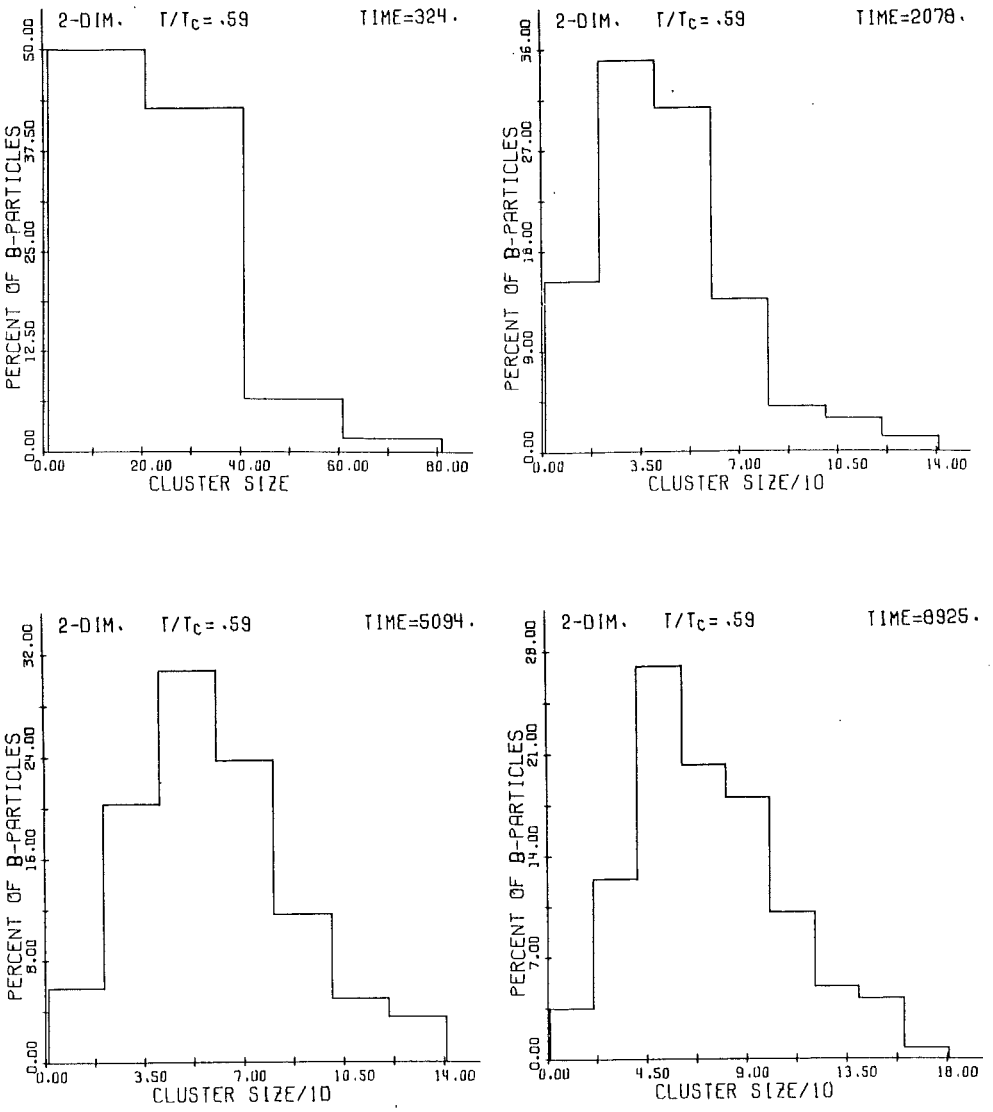

Figs. 24-27. Cluster size distribution of the two-dimensional system obtained as a combination of the results from the 200 x 200 and 80 x 80 lattices with composition c = 0.2 quenched at T = 0.6 T_c (from ref. 25).

regular (i.e., periodic) arrangement of precipitated zones, as one might expect on the basis of the simplified theory presented in the section entitled "Discussion of theoretical concepts - Macroscopic theory".

One main advantage of the Monte Carlo computer simulation method is that complications arising from additional terms in the Hamiltonian may be easily considered.

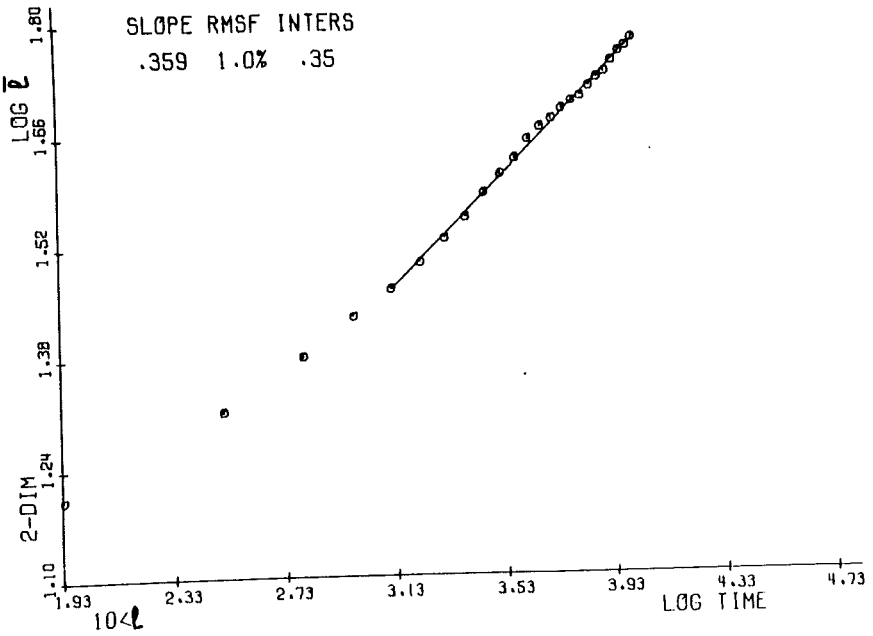

Fig. 28. Log-log plot of mean grain volume versus time for the system of Figs. 24-27 (from ref. 26).

As an example, we can treat the case where a gradient in the "field" H (Eq. 44) is present in the system. As seen from Eq. 44, such a gradient may arise if the interactions $\varphi_{AA}(\vec{r}_i,\vec{r}_j),\varphi_{BB}(\vec{r}_i,\vec{r}_j)$ do not depend only on the relative coordinate $\vec{r}_j - \vec{r}_j$, but rather on both coordinates $\vec{r}_i,\vec{r}_j$ separately. This gradient may occur, for example, in a thin film when, due to the technical production process gradients in chemical composition, lattice spacings, etc., may exist across the film. Such a case was also simulated (ref. 14) where a 55×55 lattice was used with a constant gradient ΔH in one direction. While free edges were used in the direction of the gradient, the two other edges were connected by periodic boundary conditions. Since the system is two dimensional, a thin strip rather than a thin film is represented by this choice of boundary conditions. It turns out that in such a case one obtains a more macroscopic phase separation (ref. 14), the clusters of B-atoms following the drift of the gradient and forming a coherent domain of B-phase in one part of the sample (at the bottom of the strip, for instance). This situation is illustrated in Fig. 31 where the time evolution of the local order parameter $m(x,t)$ [note that here $\underline{r} = (x,y)$, $m(x,t) = \int dy\ \Psi(\underline{r},t)$] is shown for various positions in the system. In contrast to the slow nonexponential relaxation laws discussed so far, one now observes exponential relaxation toward the equilibrium state. This behavior can be understood using the master equation (Eq. 49) from which it follows that:

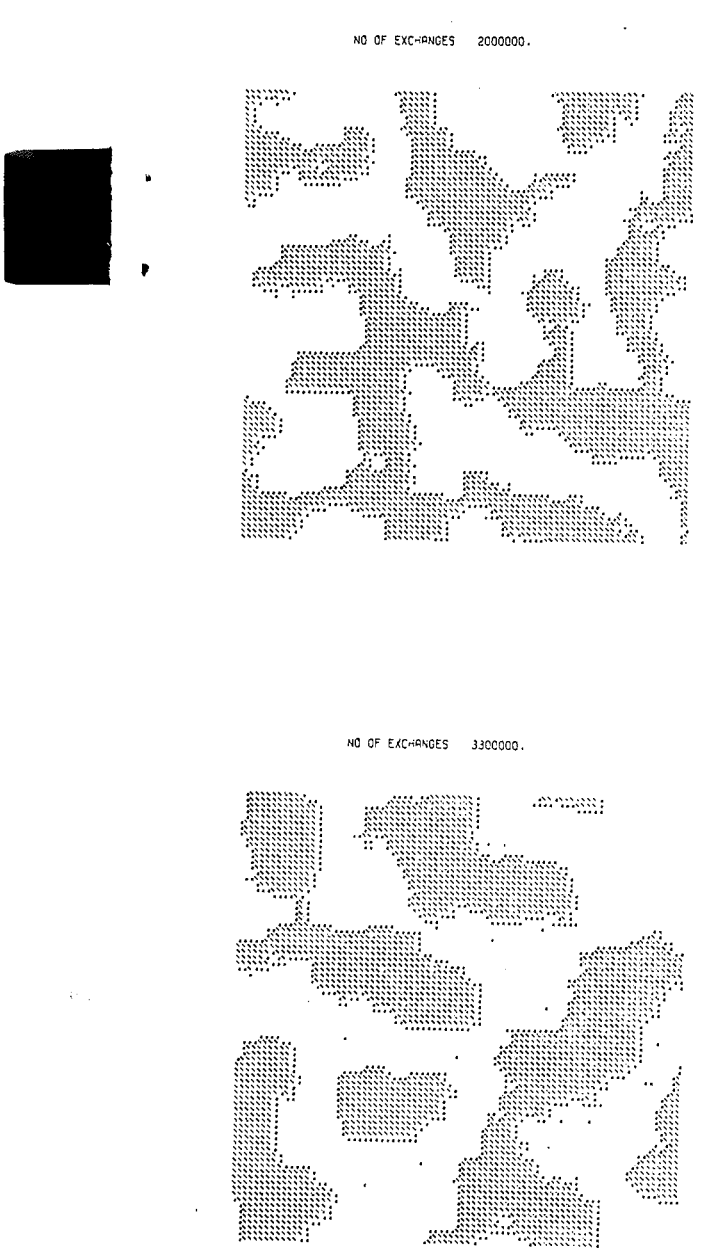

Figs. 29,30. "Snapshot pictures" of a two-dimensional 80 x 80 system with 50% A; 50% B atoms quenched at T = 0.58 T_c (from ref. 26).

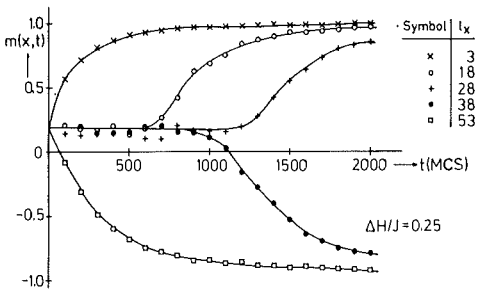

Fig. 31. Time evolution of the local order parameter m(x,t) in a system with a gradient in the field after a quench to $T = 0.5\ T_c$ (from ref. 14).

$$\frac{\partial m(x,t)}{\partial t} = -\nabla^2 \{....\} - \text{const.}\ (\Delta H)^2. \qquad (60)$$

Here, in addition to the diffusive terms (denoted symbolically by {...}, present also in the homogeneous case, one now has an extra term, const $(\Delta H)^2$, which produces the exponential relaxation.

DISCUSSION AND CONCLUSIONS

From the numerical results presented above, the following points emerge:

1. There *does not exist*, in the stochastic exchange Ising model, a time regime in which the structure function $S(\underline{k},t)$ increases exponentially with time as predicted by the linearized version of the Cahn-Hilliard theory (ref. 1-3) (see section entitled "Elementary discussion of theoretical concepts - Classical theory". On the contrary, $S(\underline{k},t)$ increases more slowly than a linear function of time, all temperatures and compositions within the coexistence curve. Hence, we conclude that the linearized Cahn-Hilliard theory, which is usually considered as a reasonable approximation for the early stages of the phase separation process, doe not provide a valid description. Of course, we have shown only that it fails with respect to the very simple stochastic Ising model considered here, but there is not reason to assume that it will work better in more complicated realistic systems. In fact, the general features of $S(\underline{k},t)$ observed experimentally (Fig. 2) and in the computer simulation (Fig. 7) are extremely similar.

2. A reasonably satisfactory description of the early stages of the phase separation process is provided by the theory of Langer, Bar-On and Miller (ref. 12) (see section entitled "Discussion of theoretical concepts - Theories including fluctuations"). This theory is constructed from a continuum description valid in the vicinity of T_c; since the critical region is not of great practical interest in the case of spinodal decomposition, it is important to note that the results of Ref. 12 provide in fact a satisfactory description of the computer simulations for temperatures as low as $T \simeq 0.6\ T_c$. This conclusion is demonstrated in Figs. 32-34,

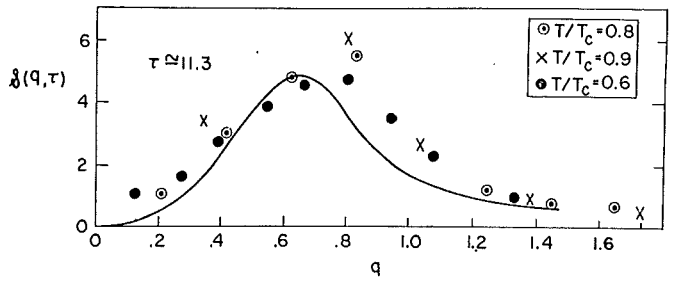

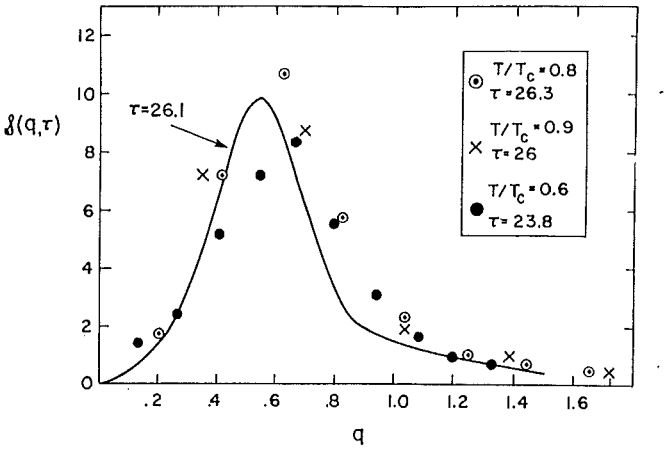

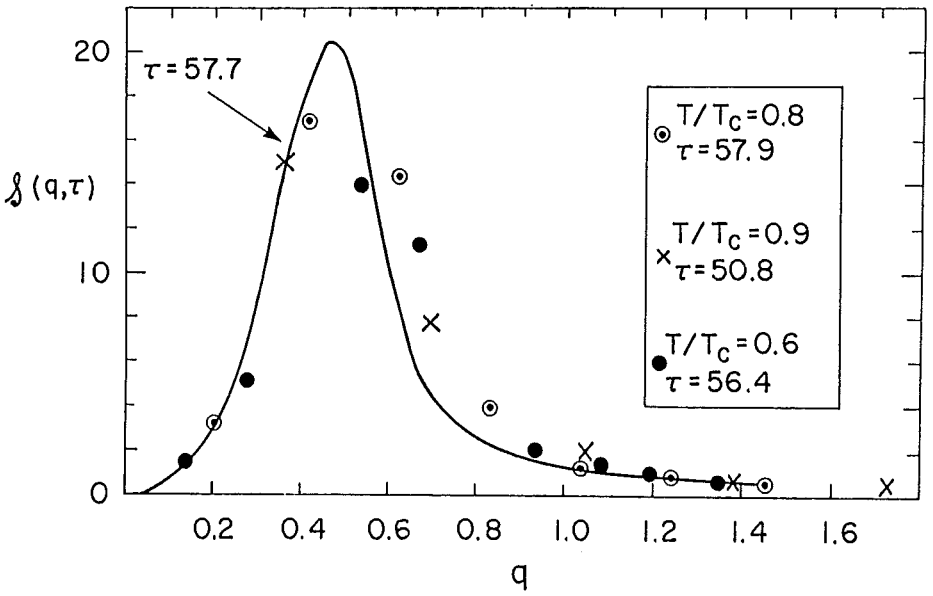

Figs. 32-34. Comparison of the computer simulation results with the calculations of Ref. 12 (solid curves) for different values of time (from ref. 25).

where the scaled structure function $\tilde{S}(q,\tau)$ is plotted; the curves are the results of the theory, while the points are the computer simulation results. This scaling expression is related to S(k,t) via the "dynamic scaling" relations (ref. 12):

$$\tau = \alpha_1(1 - T/T_c)^{\gamma + 2\nu}\, t, q = \alpha_2(1 - T/T_c)^{-\nu}\, k\ ; \tag{61}$$

$$\tilde{S}(q,\tau) = \alpha_3(1 - T/T_c)^{\gamma}\, S(k,t), \tag{62}$$

where the critical exponents (ref. 37) and other parameters were related to the independently obtained critical properties of the Ising model (ref. 12); $\gamma = 5/4$, $\nu = q/14$, $\alpha_1 = 3.51$, $\alpha_2 = 0.35$ and $\alpha_3 = 2.59$. Thus, no fitting parameter whatsoever was available in Figs. 32-34. The dynamic scaling property thus appears to hold for a surprisingly broad range of temperatures.

3. The behavior of $S(\underline{k},t)$ is qualitatively the same throughout the whole two-phase coexistence region. A well defined spinodal curve where the kinetic behavior changes abruptly does not exist in our model, and (we believe) in no other system with short range interactions. Thus, the transition from the spinodal decomposition mechanism (at large supersaturations) to the nucleation mechanism (at small supersaturations, close to the coexistence curve) is extremely gradual. This fact is also borne out by a direct study of the cluster growth processes.

4. It has been demonstrated that the time evolution of the mean cluster size as well as the particle size distribution can be studied in computer simulations. Well separated grains exist for rather low concentrations of B atoms only, however, particularly in the three-dimensional systems. Even then, the resulting cluster shapes are distinctly nonspherical and quite irregular (ref. 25). If one tries to interpret the growth of the grains in terms of a simple power law $t^{a'}$, the resulting exponent would be (a' 1/4 - 1/5) which is neither in accord with the prediction of the Lifshitz-Slyozov theory (ref. 6) (a' = 1/3) nor with Ref. 7 (a' = 1/(3+d) in d dimensions). A detailed analysis reveals, however, that an interpretation of the data in terms of a simple power law is inadequate. A more satisfactory interpretation is perhaps obtained in terms of a crossover from the slower cluster diffusion (ref. 7) to the quicker cluster evaporation (ref. 6) relaxation mechanism. This concept would imply that for large enough times the Lifshitz-Slyozov theory (ref. 6) becomes valid, but a definite conclusion concerning this point is hard to obtain, since finite size effects may affect this inference from the computer simulation. Since the late time behavior which results from the approximations of Langer, Bar-On and Miller (ref. 12) is not consistent with Ref. 6, a satisfactory theory which describes all stages of the phase separation process does not yet exist.

5. It has also been shown that the relaxation of the system is very sensitive to gradients in the interatomic forces in the system. Physically, such gradients

are expected to occur near surfaces, crystallographic grain boundaries, dislocations and crystal imperfections. It seems, on the other hand, that nonspherical clusters may appear in the system at low concentrations (ref. 25), a fact which is neglected in the interpretation of most experiments on the late stages of the evolution (ref. 5). As a consequence, great care is necessary in the interpretation of actual experiments in terms of the various theories. As we have stressed, it is one basic advantage of the computer experiments that such uncertainties about the microscopic properties of the system do not occur.

REFERENCES

1 J.W. Cahn and J.W. Hilliard, J. Chem. Phys., 28(1958)258; 31(1959)688.
2 J.W. Cahn, Acta Met., 9(1961)795.
3 For recent reviews of the Cahn-Hilliard theory of spinodal decomposition see also J.W. Cahn, Trans. Metall. Soc. AIME, 242(1968)166; H. Yamauchi and D. deFontaine, in Order-Disorder Transformation in Alloys, H. Warlimont, ed., Springer-Verlag, Berlin, 1974.
4 H. Fischmeister and G. Grimvall, in Sintering and Related Phenomena, G. C. Kuczynski, ed., Plenum Press, N. Y., 1973.
5 A.J. Ardell, in The Mechanics of Phase Transitions in Crystalline Solids, Institute of Metals Monograph Series, Vol. 33, London, 1969, p. 111; G. W. Greenwood, ibid., p. 103.
6 I.M. Lifshitz and V.V. Slyozov, J. Chem. Phys. Solids, 19(1961)35.
7 K. Binder and D. Stauffer, Phys. Rev. Lett., 33(1974)1006.
8 M.V. Smoluchowski, Phys. Z., 17(1916)385; Z. Phys. Chem., 92(1971)120; for more recent work, see, e.g., F.S. Lai, S.K. Friedlander, J. Pich and C.M. Hidy, J. Colloid Interface Sci., 39(1972)395, and references therein.
9. J.L. Lebowitz and M. Kalos, Scripta Metal., 10(1976)9, H.E. Reiss, ibid.
10 J.S. Langer, Ann. Phys. (N.Y.), 41(1967)108; 54(1969)258; J.S. Langer, Ann. Phys. (N.Y.), 65(1971)53.
11 J.S. Langer and M. Bar-On, Ann. Phys. (N.Y.), 78(1973)421.
12 J.S. Langer, M. Bar-On and H.D. Miller, Phys. Rev., A11(1975)1417.
13 J.W. Cahn, Acta Met., 14(1966)1685.
14 K. Binder, Z. Physik, 267(1974)213.
15 J.S. Langer, Acta Met., 21(1973)1649.
16 K. Binder, Phys. Rev., B8(1973)3423.
17 K. Binder and E. Stoll, Phys. Rev. Lett., 32(1973)47.
18 O. Penrose and J. Lebowitz, J. Stat. Phys., 3(1971)211; J.L. Lebowitz, Physica, 73(1974)48.
19 O. Penrose and J.L. Lebowwitz,in Studies in Stat.Mechanics, V-7, North-Holland,1978.
20 J.W. Essam, in Phase Transitions and Critical Phenomena, C. Domb and M.S. Green, eds., Vol. II, P. 197, Academic Press, New York, 1972.
21 S. Kirkpatrick, Rev. Mod. Phys., 45(1973)574.
22 H. Müller-Krumbhaar, Phys. Lett., 50A(1974)27.
23 P.A. Flinn, J. Stat. Phys., 10(1974)89.
24 A.B. Bortz, M.H. Kalos, J.L. Lebowitz and M.A. Zendjas, Phys. Rev., B10(1974)535.
25 J.Marro, A.B. Bortz, M.H. Kalos and J.L. Lebowitz, Phys. Rev., B12(1975)2000; J. Marro, Ph.D. Thesis, Yeshiva University, 1975; A. Sur, J. Marro, J. L. Lebowitz, M.H. Kalos, Phys. Rev., B15(1977)535.
26 M. Rao, J. Marro, M.H. Kalos and J. L. Lebowitz, Phys. Rev., B13(1976)7325.
27 K. Kawasaki, Phys. Rev., 145(1966)224; 148(1966)375; 50(1966)185.
28 K.B. Rundman and J.E. Hilliard, Acta Met., 15(1967)1025.
29 G.R. Speich and R.A. Oriani, Trans. AIME, 233(1965)623.
30 E.P. Butler and G. Thomas, Acta Met., 18(1970)347.
31 F. Richter, W. Bendick and W. Pepperhoff, Z. Metallide, 65(1974)32.
32 H.O.K. Kirchnev, Acta Met., 21(1973)85; Metallurgical Trans., 2(1971)2861.
33 C. Wagner, Z. Electrochemie, 65(1967)243.

34 H.E. Cook, Acta Met., 18(1970)297.
35 J.S. Langer, Physica, 73(1974)61.
36 K. Binder and D. Stauffer, in preparation.
37 C. Domb and M.S. Green, eds., Phase Transition and Critical Phenomena, Vols. I-III, Academic Press, New York, 1972-1974.
38 C.N. Yang, Phys. Rev., 85(1952)809.
39 J.W. Essam and M.E. Fisher, J. Chem. Phys., 38(1963)802,
40 K. Binder, in Nucleation, Vol. II; A. C. Zettlemoyer, ed., Elsevier, 1977.
41 K. Binder and H. Müller-Krumbhaar, Phys. Rev., B9(1974)2328.
42 For a general discussion of the Monte Carlo method and for references, see, e.g., H. Müller-Krumbhaar and K. Binder, J. Stat. Phys., 8(1973)1. Applications to spin-exchange problems are treated in Refs. 14, 12, 14-26, 43.
43 A.B. Bortz, J. Stat. Phys., 11(1974)181.
44 A.B. Bortz, M.H. Kalos and J.L. Lebowitz, J. Comput. Phys., 17(1975)10.
45 M.E. Fisher, in Critical Phenomena, M.S. Green, ed., Academic Press, New York, 1971.
46 K. Binder, Physica, 58(1972)62; K. Binder, in Phase Transitions and Critical Phenomena, Vol. V, C. Domb and M.S. Green, eds.
47 For reviews of nucleation theory, see, e.g., A. C. Zettlemoyer, ed., Nucleation, M. Dekker, New York, 1969, and other chapters of this book.
48 This point can even be seen from the point of view of the Cahn-Hilliard theory outlined in Section III, if one uses a free energy expression like Eq. 5 to calculate the formation energy of droplets. It turns out that this formation energy becomes very small (and the resulting droplets become diffuse) as one reaches the spinodal line, indicating that there is a rather smooth transition only. See J.W. Cahn and J.E. Hilliard, J. Chem. Phys., 31(1959)688 for a more detailed discussion.